



# HHS Public Access

Author manuscript

*Adv Mater.* Author manuscript; available in PMC 2020 June 01.

Published in final edited form as:

*Adv Mater.* 2019 June ; 31(23): e1900332. doi:10.1002/adma.201900332.

## Two-Dimensional Nanoclay for Biomedical Applications: Regenerative Medicine, Therapeutic Delivery, and Additive Manufacturing

**Dr. Akhilesh K. Gaharwar [Prof.],**

Biomedical Engineering, Dwight Look College of Engineering, Texas A&M University, College Station, TX 77843

Material Science and Engineering, Dwight Look College of Engineering, Texas A&M University, College Station, TX 77843

Center for Remote Health Technologies and Systems, Texas A&M University, College Station, TX 77843

**Dr. Lauren M. Cross,**

Biomedical Engineering, Dwight Look College of Engineering, Texas A&M University, College Station, TX 77843

**Dr. Charles W. Peak,**

Biomedical Engineering, Dwight Look College of Engineering, Texas A&M University, College Station, TX 77843

**Karli Gold,**

Biomedical Engineering, Dwight Look College of Engineering, Texas A&M University, College Station, TX 77843

**Dr. James K. Carrow,**

Biomedical Engineering, Dwight Look College of Engineering, Texas A&M University, College Station, TX 77843

**Anna Brokesh,** and

Biomedical Engineering, Dwight Look College of Engineering, Texas A&M University, College Station, TX 77843

**Kanwar-Abhay Singh**

Biomedical Engineering, Dwight Look College of Engineering, Texas A&M University, College Station, TX 77843

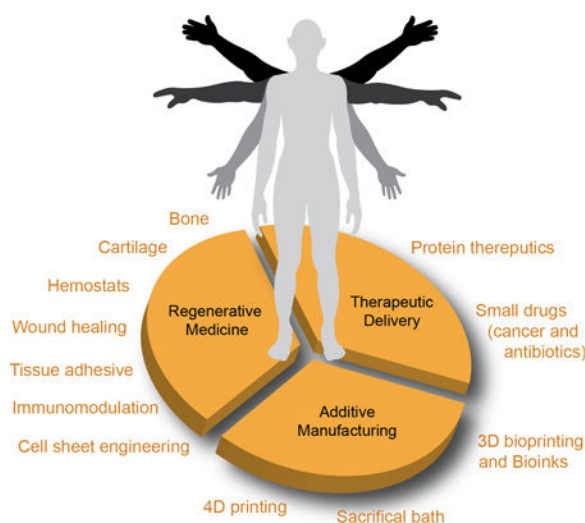
### Abstract

Clay nanomaterials are an emerging class of two-dimensional (2D) biomaterials of interest due to their atomically thin layered structure, discotic charged characteristics and well-defined composition. Synthetic nanoclays are plate-like polyions composed of simple or complex salts of silicic acids with a heterogeneous charge distribution and patchy interactions. Due to their biocompatible characteristics, unique shape, high surface-to-volume ratio and charge distribution, nanoclays are investigated for various biomedical applications. This review article will provide a critical overview of the physical, chemical and physiological interactions of nanoclays with

biological moieties including cells, proteins and polymers. The state-of-the-art biomedical applications of 2D nanoclay in regenerative medicine, therapeutic delivery and additive manufacturing are reviewed. In addition, recent developments that are shaping this emerging field are discussed and promising new research directions for 2D nanoclay-based biomaterials are identified.

## Graphical Abstract

The biomedical applications of emerging class of two-dimensional (2D) nanoclay in regenerative medicine, therapeutic delivery and additive manufacturing are reviewed. A critical overview on physical, chemical and physiological interactions of nanoclay with biological moieties including cells, proteins and polymers are discussed. In addition, recent developments that are shaping this emerging field are examined and promising new research directions for 2D nanoclay-based biomaterials are identify.



## Keywords

Laponite® nanoclay; nanosilicates; two-dimensional (2D) nanomaterials; tissue engineering; 3D printing and bioprinting; drug delivery

## 1. Introduction

Clays have been used throughout history as a bioactive agent, dating back to 2500 BC, where the *clay plates of Nippur*, Mesopotamia, documented the use of clays to treat wounds and inhibit hemorrhages. The distinguished *Papyrus Ebers*, dating back to 1600 BC, also describes the use of clay-based materials as remedies for diarrhea, dysentery, tapeworm, hookworm, and wounds. In addition, clay-based materials have been used throughout history for intestinal ailments, fever treatments, antiseptics, remedies for skin afflictions, and anti-inflammatories for mummification. From Ancient Greece through to Roman times, Medieval periods, and the present-day, clay and clay-based materials have been used in food science, nutritional applications, cosmetics, healthcare products, and most recently in the

biomedical sciences. Aside from therapeutic applications, the diversity of clay structures and properties permits their use as stabilizer and/or reinforcing agents, as well as representing a major constituent of plastics, paints, paper, rubber, and cosmetics.

Clays are composed of finely-grained, layered individual particles that are typically derived from naturally occurring sources featuring one or more phyllosilicate mineral.<sup>[1]</sup> Phyllosilicate minerals are composed of a silicate crystal structure with various other elemental compositions and physical dimensions.<sup>[2]</sup> Although clays possess octahedral and tetrahedral sheets as basic building blocks, their specific structures and compositions categorize them into different families, such as kaolinite, smectite (or bentonite), and palygorskite-sepiolite.<sup>[3]</sup> In addition, the composition and properties of clays derived from natural sources vary considerably depending on their geological origin. To overcome the inhomogeneity of natural clays, the use of synthetic mineral clays has gained popularity for biomedical applications as they are readily produced in large quantities with highly controlled composition and properties.

Laponite® nanoclay, a trioctahedral smectite, is a unique additive composed of layered synthetic silicate synthesized from inorganic mineral salts. This two-dimensional (2D) nanoclay is characterized by the empirical formula  $(\text{Na}^{+}_{0.7}[(\text{Si}_8\text{Mg}_{5.5}\text{Li}_{0.3})\text{O}_{20}(\text{OH})_4])^{-0.7}$  with disk-shaped geometry of 20–50 nm diameter and 1–2 nm thickness. Given this unique composition and size, this nanoclay exhibits dual charge distribution, i.e. permanent negative charge on surface of the particle and a positive charge along the edges (Fig. 1a). Although the first paper on Laponite® nanoclay was published in 1969 (according to ISI Web of Science), it was not until the early 21<sup>st</sup> century that an exponential increase in the number of publications and citations related to Laponite® nanoclay occurred (Fig. 1b, searches used the following keywords: laponite(s) or nanoclay(s) or nanosilicate(s), which are often used interchangeably). From this literature search, we observe that Laponite® nanoclay is extensively used in numerous fields to improve the structure, property and performance of a wide variety of products as a rheological modifier (e.g. household cleaning products, toothpastes, or personal care products) or to aid in film formation (e.g. adhesives, paints, automotive coatings, wood coatings, or ceramic glazes).<sup>[4]</sup> In this article, we will specifically focus on biomedical applications of Laponite® nanoclay. The hydrophilic characteristics and high surface area of Laponite® nanoclay facilitate physical interactions with a range of small and large biomolecules, and thus have been extensively investigated in the fields of regenerative medicine, therapeutic delivery, and additive manufacturing (Fig. 1c), which will be the primary focus of this article.

In this review, we focus on the current and emerging applications of Laponite® nanoclay (henceforth referred to as simply *nanoclay*), specifically highlighting recent advances that pioneer the use of nanoclay in biomedical applications. First, we critically review the unique physical structure, shape, and chemical compositions of nanoclay that permits wide-spread application. Additionally, we discuss the use of nanoclay to direct cell behavior, interact with physiological environments, sequester therapeutics molecules, and act as a rheological aid in 3D printing. Some of the emerging applications of nanoclay will also be described. Specifically, the current state of nanoclay research in the field of biomedical and bioengineering will be discussed followed by identification of emerging research directions.

## 2. Physical Structures, Shape and Chemical Composition of Laponite® Nanoclay

The manufacturing process of nanoclay results in various sizes and chemical compositions, but Laponite® nanoclay is broadly categorized as a synthetic smectite clay. Analogs of Laponite® are the natural clay mineral hectorites, which are a part of a wider phyllosilicate (or sheet silicates) group including Kaolinite, Montmorillonite, and Vermiculite. Compared to natural clays, Laponite® nanoclay has low heavy metal content, but has a structural composition consisting of an octahedral sheet of magnesium oxide between two parallel tetrahedral sheets of silica. The empirical formula of Laponite® nanoclay (the most widely studied Laponite for biomedical applications)  $(\text{Na}^{+}_{0.7}[(\text{Si}_8\text{Mg}_{5.5}\text{Li}_{0.3})\text{O}_{20}(\text{OH})_4]^{-0.7})$  suggests that lithium ions substitute a small amount of magnesium ions within the octahedral middle sheet. Rockwood Chemicals (Gonzales, TX) and LaPorte Industries (Birmingham, UK) were the first to develop Laponite® nanoclay by controlling chemicals formulations, temperatures and pressures.<sup>[5]</sup> Through this process, size, shape, and chemical composition can be tightly controlled in comparison to naturally occurring clays.

### 2.1 Exfoliation of Nanoclay

Aqueous exfoliation of nanoclay is commonly used for biological applications, while organo-exfoliation can be useful in creating stable, self-assembled hydrogels. During the exfoliation process, nanoclay undergoes physical re-arrangement, or “aging”, over a period of hours to months, depending on the concentrations of nanoclay.<sup>[6, 7–9]</sup> During the manufacturing process of nanoclay, a sodium ion is adsorbed onto the exterior surface of the tetrahedral silica sheet. Due to electrostatic interactions in dry environments, it is most energetically favorable for the sodium cation to be shared between multiple nanoclay sheets, causing the formation of nanoclay tactoids or stacks of particles (Fig 2a). The nanoclay sheets are stabilized *via* ionic bonding; individual clay layers are held together *via* van der Waals forces giving rise to systemic “*d-spacing*”.<sup>[9]</sup> Scattering techniques are often used to measure the “*d-spacing*”, where an increase in *d-spacing* indicates an intercalated tactoid nanoclay.<sup>[10, 11]</sup>

For exfoliation to occur, individual platelets must be separated. Previous reports suggest that tactoids are completely exfoliated within 4 hours at a concentration of 1.5 wt% in water.<sup>[12]</sup> Sodium cations have a preference to be surrounded by 5–6 water or hydroxide molecules, and this hydration of the sodium cation results in an increase in osmotic pressure on the interior of the tactoid, weakening the initially layered structure. Transmission electron microscopy images have shown diameter of individual nanoclay ~20–50 nm and atomic force microscopy have shown a thickness of 1–2 nm (Fig 2b).<sup>[13]</sup> Due to random thermal motions of the nanoclay and charge distribution, the individual nanoclay sheets begin to orient in an edge-to-face arrangement that allows for faster exfoliation. Increased nanoclay concentrations exfoliate faster due to the formation of a macroscopic network that holds the individual sheet in position with electrostatic forces, while the tactoid exfoliates. Detailed discussion regarding the intercalation and exfoliation of nanoclay can be garnered from the appropriate literature.<sup>[9, 14, 15]</sup>

In biological solution (aqueous), exfoliation of nanoclay depends strongly on the presence of ions and protein. Depending on the charge characteristics of these ions or protein, exfoliation of nanoclay can be facilitated or hindered. For example, presence of serum protein in solution will strongly interact with nanoclay tactoid and will result in partial exfoliation of nanoclay. A recent study has highlighted the influence of serum protein on the formation of stable nanoclay solution, as nanoclay electrostatically interacts with protein to form a nanoclay-protein complex.<sup>[16]</sup> Functionalization of the nanoclay surface can be used to facilitate interaction with polymer or biomolecules;<sup>[17]</sup> however, surface functionalization processes are cumbersome and time consuming. Due to the recent emergence of nanoclay for biomedical applications, limited studies have been performed to explore aqueous exfoliation of nanoclay in biologically relevant fluids such as cell culture media, serum solution or phosphate buffer saline.<sup>[16]</sup>

Organic polymers and epoxies are alternatives to aqueous solvent for nanoclay exfoliation.<sup>[18]</sup><sup>[19]</sup> Using small and wide-angle x-ray diffraction, researchers have shown the exfoliation of nanoclay using quaternary alkylammonium ions.<sup>[20]</sup> Others have hypothesized that epoxy curing generates elastic forces that are responsible for exfoliation of the clay structures.<sup>[21]</sup> The separation of the tactoid structures appears to begin with separation of the outermost layers due to an imbalance between free-ion and paired-ion energies.<sup>[21]</sup> However, as many epoxies and polymers are hydrophobic, nanoclay itself must first be rendered hydrophobic. This can occur through a cation exchange process in which sodium cations are exchanged for organic chain molecules. Using cetyltrimethylammonium bromide (CTAB) at 3–4 times the amount of the cation exchange capacity of nanoclay, the ammonium cation of CTAB will replace the native sodium cation after approximately 12 hours.<sup>[22]</sup> Once the sodium cation is replaced, hydrophobic organic polymers such as polystyrene can easily incorporate exfoliated nanoclay, resulting in a microcomposite solution of nanoclay aggregates surrounded by polymer.<sup>[23]</sup> Use of amphiphilic polymers and solvents are also reported for nanoclay exfoliation. For example, combination of chloroform and ethanol in ratio of 90:10 has been described as an optimal concentration for nanoclay exfoliation.<sup>[24]</sup>

## 2.2 Phase Diagram and Patchy Interactions.

Nanoclay has a complex phase diagram.<sup>[8]</sup> After exfoliation in aqueous solution, nanoclay orders into complex internal arrangements. In turn, these internal arrangements result in macroscopic solutions that range from low viscosity solutions to highly ordered colloidal gels and Wigner glasses (Fig 2c).<sup>[8]</sup> As a synthetic material, the size, shape, and chemical makeup of nanoclay are precisely controlled during the fabrication process, making Laponite® nanoclay a model system to investigate clay phase diagrams. There is extensive, ongoing research to determine the effect of nanoclay concentration on the formation of internal structures.<sup>[12, 25]</sup> Upon exfoliation or hydration, it is suggested that nanoclay form T-bonded clusters with a wide-spread “*house-of-cards*” structure.<sup>[12, 26]</sup> This particular internal structure has been previously studied *via* multiple scattering techniques including dynamic light scattering (DLS)<sup>[14, 27, 28]</sup>, small-angle neutron scattering (SANS)<sup>[29]</sup> and x-ray scattering.<sup>[30]</sup> It is important to note that external factors such as temperature, salt concentration, and ion concentration will also significantly influence the aging process of nanoclay solution. Nanoclay aging is a direct result of the intercalation and exfoliation of

individual clay sheets. At low ion concentrations ( $<10^{-4}$  mM), nanoclay remains stable in solution and interacts in the aforementioned “*house-of-cards*” structure.<sup>[12, 31]</sup> With addition of external ions (i.e. salt) or polymer, or changes in pH, the subsequent interactions and phase diagram are less well defined.<sup>[9, 31–33]</sup>

Earlier studies have extensively investigated the phase diagram of “neat” or “pure” nanoclay. [8, 9, 11, 12, 26, 31, 33] At low external ionic concentrations, nanoclay forms an isotropic liquid (up to 2 wt./wt.%). This phase is characterized by nanoclay being fully exfoliated, but not interacting with each other.<sup>[7–9]</sup> At 2–3 wt.% of nanoclay, isotropic gels are formed where nanoclay are partially interacting in a “*house of cards*” structure. Above 3 wt./wt.%, nanoclay forms nematic gels (liquid crystals). During this phase, exfoliated nanoclay forms a tightly packed “*house-of-cards*” structure with minimal nanoclay movement, which are referred to as shake gels or empty glass (Wigner glass) phase. Each of these phases have been extensively investigated using various techniques such as birefringence experiments, SANS, and SAXS.<sup>[7–9]</sup> Earlier studies have demonstrated that the phase diagram of nanoclay depends on concentration, temperature, salt concentration, and ion concentration. [7–9, 14, 27, 34] The addition of salt, specifically monovalent and divalent cations, strongly influences the internal structures of nanoclay gels. Cations interact with Laponite, influencing the electrical double layer formation; for example, monovalent cation ( $\text{Na}^+$ ) released from the surface due to osmotic pressure can facilitate nanoclay exfoliation. The addition of small amount of salts ( $<10^{-2}$  M) prevents the sodium cation from releasing, thus preventing nanoclay exfoliation. At higher salt concentrations ( $>10^{-2}$  M), flocculation of nanoclay can be observed due to the disruption of the electrical double layer. This results in enhanced face-to-face alignment of nanoclay and the formation of aggregates. Monovalent cations (e.g.  $\text{Na}^+$ ) result in the largest “d-spacing” between nanoclay sheets ( $\sim 3.6$  nm).<sup>[35]</sup> Use of higher valency cations, such as divalent and trivalent, reduces the d-spacing between nanoclay. Structural analysis *via* SAXS indicates that nanoclay exposed to multivalent cations results in higher number of particles present in the solution.<sup>[35]</sup>

Experimental results often report the physical-chemical relationship between nanoclay shape and chemical composition. The edges of nanoclay are positively charged due to cleaved  $\text{Mg}^{2+}$  or  $\text{Li}^{2+}$  exposure to an aqueous environment, while the face of nanoclay is negatively charged because of the presence of oxygen on the surface. Due to the unique charge distribution, particles orient themselves in such a manner that the positively charged edge interacts with the negatively charged face. The orientation of particles have been modeled through Monte Carlo simulations with various phase diagrams proposed for nanoclay.<sup>[36, 37]</sup> These models rely on correct mathematical descriptions of the nanoclay system.

Overall, the nanoclay-nanoclay interactions are essential for understanding how nanoclay may respond to the addition of other elements such as polymer, protein or cells/tissue environment. We will now examine each of these environments in detail.

### 3. Laponite® Nanoclay in Physiological Environments

Many of the forces that dictate nanoclay interactions are also responsible for the internal organization in aqueous environments. The dynamics of this organization are highly

dependent on multiple conditions including temperature, pH, ionic strength, the presence of soluble ions/proteins, and nanoclay concentration.<sup>[9, 34, 38]</sup> Due to the complexities of this process, many studies have investigated the role of each parameter independently as it pertains to nanoclay phase diagrams.<sup>[7, 12, 14, 26, 36]</sup> In water (pH~10), exfoliated nanoclay forms empty glass (Wigner glass) phase due to the predominant negative charges. As soon as this exfoliated nanoclay is subjected to solution containing ions or proteins, flocculation occurs near the gel-solution interface (Fig. 3).<sup>[39]</sup> Flocculation is primarily driven by the formation of an electric double layer and electrostatic interactions between nanoclay due to the introduction of ions and/or proteins. This double layer acts as a protective shield, providing physical and chemical stability to the exfoliated glass phase. It is possible that ions or protein present in the double layer might slowly migrate towards interior gels. In addition to the formation of structures within physiological aqueous environments, nanoclay will dissociate during the aging process at lower pH (<10). This dissociation not only modifies the physical properties of the nanoclay, but may also be responsible for directing a variety of changes in the surrounding microenvironment. Specifically, the ability of nanoclay to arrange in multiple configurations such as exfoliated or intercalated structure, and the “*house-of-cards*” arrangements, will directly influence its interactions with cells, biomolecules, and polymers. We will review the various parameters responsible for the nanoscale arrangements between nanoclay and how these structures, or lack thereof, impact material and biological behavior at the nano-, micro- and macro- scales.

### 3.1 Structural Stability and Ionic Dissociation of Laponite® Nanoclay

Nanoclay ( $\text{Na}^{+}_{0.7}[(\text{Mg}_{5.5}\text{Li}_{0.3})\text{Si}_8\text{O}_{20}(\text{OH})_4]^{-0.7}$ ) is composed of layered structures of octahedral magnesium and lithium ions sandwiched between tetrahedral silicon ions. Accordingly, the expected composition of nanoclay is oxygen (62.34%), silicon (20.78%), magnesium (14.29%), sodium (1.81%), and lithium (0.78%). This stoichiometry is validated experimentally *via* inductively-coupled mass spectrometry (ICP-MS). The isoelectric point of nanoclay is pH ~10;<sup>[9, 34]</sup> at higher pH, nanoclay exhibits stable structure, while at lower pH (<9) chemical dissolution of individual particles is observed. Several studies have investigated the stability of nanoclay from the perspective of Brønsted-Lowry acids and bases, as nanoclay has demonstrated notable pH-buffering capabilities.<sup>[9, 34]</sup> It has been shown that nanoclay dissociates into non-toxic ionic products ( $\text{Na}^{+}$ ,  $\text{Mg}^{2+}$ ,  $\text{Si}(\text{OH})_4$ ,  $\text{Li}^{+}$ ) below pH ~9.<sup>[9, 40]</sup> After nanoclay disperses in water (pH<9),  $\text{OH}^{-}$  ions dissociate from the edge to re-establish basic pH.<sup>[40]</sup> During this stabilization process, lithium ion release may occur more rapidly than magnesium or silicon ion release. In addition, monovalent lithium is less stable than divalent magnesium or tetravalent silicon, therefore contributing to the rapid increase in lithium release. Contrary to lithium dissociation, silicon ions release faster compared to magnesium at lower pH, as silicon ions are present on the outer layer and are more susceptible to dissociation. The leaching of ions from the nanoclay is a time-dependent process (aging) and can be modulated by solution pH, temperature and nanoclay concentrations.

As most biological systems are highly buffered, ions released from nanoclay may elicit strong cellular or extracellular influence. For example, nanoclay dissociation near the cell membrane can disrupt or alter various ion channels. Following cellular internalization,

nanoclay is subjected to acidic intracellular vesicles during cellular trafficking, activating intracellular release of ions. The ion release can result in the generation of reactive oxygen species (ROS), which further facilitates nanoclay dissociation. Additionally, an increase in local ion concentration will increase the attractive forces between nanoclay, thereby leading to more rapid aging or dissociation.<sup>[7, 8, 38, 41]</sup> Future work is required to relate these physicochemical results with cellular outcomes, particularly in understanding cell signaling due to internalization of nanoclay as well as the effect of released ions on cellular functions.

The presence of soluble  $Mg^{2+}$ ,  $Li^+$ , and  $Si(OH)_4$  following dissolution of the nanoclay may control a variety of cell processes. Specifically, earlier studies have demonstrated that  $Mg^{2+}$  ions play a role in cell adhesion through enhancing interactions with integrin biomolecules.<sup>[42]</sup> This complements the ability of these particles to form a protein corona, improving interactions at the cellular membrane. Additionally, divalent ions like  $Mg^{2+}$  assist in the polymerization of actin fibers throughout the cytoplasm.<sup>[43]</sup> Interestingly, whole-transcriptome analysis of nanoclay-treated human mesenchymal stem cells (hMSCs) demonstrated differential expression related to actin polymerization and mobility, potentially due to the presence of  $Mg^{2+}$ .<sup>[13]</sup> Next,  $Li^+$  activates Wnt-responsive genes by elevating cytoplasmic  $\beta$ -catenin<sup>[44–46]</sup> and Wnt signaling in turn stimulates osteogenesis as well as glycosaminoglycan synthesis *in vivo* and *in vitro*, respectively.<sup>[44, 47]</sup> Lastly, Si and  $Si(OH)_4$  are essential for metabolic processes, angiogenesis during bone regeneration, and calcification of bone tissue.<sup>[48, 49]</sup> The inherent bioactivity of these soluble ions may point to potential regenerative engineering applications of nanoclay, which have not yet been explored. As use of nanoclay increases within the biomedical industry, additional experimentation is desirable to probe the effect of ionic dissolution products of nanoclay on cellular functions.

### 3.2 Interactions of Laponite® Nanoclay with Proteins

The structural characteristics of nanoclay impact biological behavior at multiple length scales including cellular internalization, retention, cytocompatibility, immunomodulatory properties, bioactivity and biocompatibility. Nanoclays have high surface area due to disc-shaped morphology and dual charged surface characteristics, facilitating facile interactions with a range of proteins. A recent study has shown that after mixing nanoclay with cell culture media containing serum, a significant increase in hydrodynamic diameter ( $D_H$ ) from ~45 nm to ~90 nm and a decrease in zeta potential ( $\zeta$ ) from -40 mV to -25 mV are observed.<sup>[13]</sup> These results indicate that serum protein is physically adsorbed on nanoclay surface *via* electrostatic interactions. The adsorption of protein onto nanoparticle surfaces dictate nanoparticle- cellular interactions.<sup>[50]</sup> Specifically, the localization of proteins at the cell surface may promote activation of a variety of cell machinery, which initiates the nanoparticle internalization.

The specific nanomaterial properties that govern their coating by target proteins in the surrounding media are not clearly identified; however, the chemical composition, surface area-to-volume ratio, charge, and size are known to play key roles.<sup>[51]</sup> For example, formation of a protein corona will strongly depend on shape and surface energy. Depending on the specific charge distribution across a protein, it can adsorb on either the positively



charged edge or the negatively charged surface of a nanoclay (or both). In a recent report, it was shown that proteins preferentially attach to the edge of nanoclays.<sup>[52]</sup>

In addition, the size of nanoclay is also expected to influence the formation of protein-nanoclay complex, which will dictate biological response to nanoclay. Unfortunately, the composition of proteins that coat the nanoclay surface over time, in consideration of the Vroman effect, has yet to be investigated. From previous studies, we can formulate a hypothesis regarding the formation of “hard” and “soft” protein coronas when nanoparticles are exposed to physiological fluids.<sup>[53]</sup> Protein conformation on the nanoclay surface will determine subsequent binding to cell membrane receptors. The maintenance of native protein structure enables more targeted binding to specific receptors, which is relevant for nanoclay internalization. Furthermore, the makeup of coated proteins will also define biomedical applications of nanoclay in tissue engineering and therapeutic delivery.

#### 4. Cytocompatibility of Laponite® Nanoclay and Interactions with Cells

The cytocompatibility of nanoclay has been investigated using a range of biochemical assessments, such as monitoring cell viability, cytoskeletal organization, metabolic activity and cell cycle. Direct exposure to increasing concentrations of nanoclay was used to determine the half maximal inhibitory concentration (IC<sub>50</sub>). This study demonstrated that the cell metabolic activity was not significantly affected by the addition of nanoclay at lower concentrations (<1 mg/mL) and IC<sub>50</sub> was observed at 4–5 mg/mL for both hMSCs and preosteoblasts.<sup>[54]</sup> Compared to other types of nanoengineered materials, the IC<sub>50</sub> for nanoclay is 2–10 fold higher, indicating high cytocompatibility. No significant production of reactive nitrogen species (RNS) and reactive oxygen species (ROS) were observed at a lower concentration (100 µg/mL).<sup>[54]</sup> These observations were validated using a lactose dehydrogenase (LDH) assay that monitors cell membrane integrity, and an Alamar blue assay that monitors mitochondrial activity.<sup>[13]</sup> The nanoclay treatment also did not show a significant effect on cytoskeletal organization compared to untreated cells.<sup>[54]</sup> In addition, when treated with <100 µg/mL nanoclay, the majority of cells were observed in G1 and G2 phases.<sup>[13]</sup> These studies highlight that nanoclays are compatible with mammalian cells and do not adversely affect cell functions during direct exposure.

As soon as nanoclays are introduced to *in vitro* and *in vivo* environments, the formation of a protein corona on the nanoclay surface is expected to facilitate receptor-mediated endocytosis.<sup>[55]</sup> Receptor-mediated binding of surface-adsorbed proteins initiate a cascade of events inside the cell, including internalization of protein-coated nanoclay (Fig. 4a).<sup>[13]</sup> Earlier studies have shown that nanoclay readily attaches (within <5 mins) to the cell surface as visualized by hyperspectral imaging, confocal microscopy, and flow cytometry.<sup>[13]</sup> The internalization of nanoclay *via* various mechanism has been investigated by blocking different endocytic pathways such as clathrin, caveolar, and micropinocytosis with inhibitory drugs.<sup>[55],[13]</sup> A significant reduction in cellular internalization (~80%) of nanoclay was observed in the presence of clathrin-inhibitor (chlorpromazine hydrochloride). Alternatively, other endocytic mechanisms, such as macropinocytosis (wortmannin) and caveolar-mediated (nystatin), were less prominent in nanoclay uptake. The rapid internalization of nanoclay (within 5 mins) was observed *via* flow cytometry, which further validated clathrin vesicle

dynamics<sup>[56]</sup>. Subsequently, nanoclay are trafficked to lysosomal vesicles following cellular internalization.<sup>[13]</sup>

To understand the interaction of nanoclay with cells at the whole transcriptome level, RNA-sequencing was performed on nanoclay-treated hMSCs compared to a control of untreated hMSCs. Interestingly, nanoclay differentially regulated more than 4000 genes, suggesting a widespread cellular response (Fig. 4b).<sup>[13]</sup> By clustering highly expressed genes into different cellular processes, nanoclay treatment significantly enriched various biological process including protein targeting to membrane (GO:0006612), cellular response to growth factor stimulus (GO:0071363), endochondral bone growth (GO:0003416), cell morphogenesis involved in differentiation (GO:0000904), positive regulation of MAPK cascade (GO:0043410), cWnt signaling pathway (GO:0060070), BMP signaling (GO:0030509), TGF- $\beta$  receptor signaling pathway (GO:0007179), and notch signaling pathway (GO:0007219).<sup>[13]</sup> These pathways play important roles in various cellular functions including proliferation, migration, multipotency, and production of extracellular matrix,<sup>[46, 57]</sup> indicating nanoclay exposure affects these processes. The GO enrichment analysis suggests that the nanoclay treatment predominantly influences kinase activity, basic cell processes, endocytosis, and stemness/regenerative capacity (Fig. 4c).<sup>[13]</sup>

For many nanoparticles, the generation of reactive oxygen species (ROS) is a key contributor to nanotoxicity. While ROS production occurs naturally in cellular systems, over production can lead to process dysfunction and ultimately cell death. An increase in ROS production is observed with an increase in nanoclay concentration.<sup>[54]</sup> Generation of ROS typically activates a variety of cellular pathways, including mitogen activated protein kinase (MAPK) cascades (Fig. 4d).<sup>[13]</sup> Signaling within the stress-responsive pathway of MAPK often occurs to mitigate ROS damage. Transcriptomic analysis indicated activation of both stress- and receptor-responsive MAPK pathways. The crosstalk between these pathways from a variety of transcription factors may enable ROS to play role in downstream signaling for proliferation and/or differentiation of cells. This cellular effect of nanoclay needs to be investigated in detail using different cell types to explore its potential in various tissue engineering applications.

## 5. Laponite® Nanoclay-Polymer Interactions

Nanoclay solutions exhibit complex phase behavior and the addition of polymers to nanoclay solution further complicates the sol-gel behavior, presenting new challenges in determining precise interactions between nanoclay and polymer chains. For example, these adsorbed polymer chains can have different regions, such as tails, trains, and loops (Fig. 5a). The exact interactions between nanoclay and polymeric chains are unknown, but it is hypothesized that electrostatic interactions and hydrogen bonding may play significant roles.<sup>[8, 9]</sup> Therefore, charged groups present on a polymeric backbone may interact with charged surface/edge of nanoclay *via* electrostatic interactions. In order for chemical interactions to occur, the use of active end groups such as dopamine<sup>[58, 59]</sup> or siloxane<sup>[60]</sup> on polymer chains are required to form covalent bonds with nanoclay surfaces. In such cases nanoclays act as crosslink epicenters, where a single particle connects to multiple polymeric chains and reinforces the network.

Polymer structure, molecular weight, type of pendant group, temperature, and hydrophilicity define nanoclay-polymer interactions.<sup>[61, 62]</sup> For example, shorter polymer chains (i.e., polymer with low molecular weight) can be physically adsorbed onto nanoclay surface. As we increase the polymer molecular weight, polymer tails bridge between multiple nanoclay resulting in the formation of a physically crosslinked network (Fig. 5b). If polymer chains are physically adsorbed without formation of covalent bond, the resulting solution will have shear-thinning characteristics imparted by nanoclay. Several in-depth reviews are available on understanding polymer-nanoparticles interactions<sup>[63]</sup>, thus we will limit the following discussion to few biologically relevant systems.

The ability of nanoclay to modify the rheological properties of synthetic and natural polymers has been widely investigated.<sup>[64, 65]</sup> It is well established that the addition of small amounts of nanoclay to polymeric binder forms shear-thinning hydrogels<sup>[66]</sup>, which are extensively used in the biomedical discipline for cells and therapeutic delivery, tissue regeneration, and adhesives<sup>[67]</sup>. Hydrogels are 3D crosslinked networks of polymers capable of absorbing large amounts of water (>80%) while maintaining physiological stability and structural integrity.<sup>[68]</sup> Shear-thinning hydrogels possess a high viscosity at low shear rates, but readily flow upon exposure to high shear rates or stresses.<sup>[69, 70]</sup> The anisotropic charge distribution on the nanoclay (positive edges, negative faces) results in formation of a “*house-of-cards*” structure, which contributes to the shear-thinning properties of nanoclay-polymer solutions (Fig. 5c).<sup>[71]</sup> Specifically, the electrostatic interactions are reversible in nature and can break and reform by applying mechanical stress and relaxation to the system, respectively.

A range of synthetic and natural polymers including poly(ethylene glycol/oxide) (PEG/PEO),<sup>[61, 72–74]</sup> pluronics,<sup>[75]</sup> poly(N-isopropylacrylamide) (PNIPAM),<sup>[76]</sup> gelatin,<sup>[77]</sup> or kappa-carrageenan (kCA)<sup>[78]</sup> have been combined with nanoclay to obtain nanocomposites for biomedical applications. The interactions of linear synthetic polymers, such as PEG/PEO<sup>[73, 79, 80]</sup> and PNIPAM,<sup>[81, 82, 83]</sup> with nanoclay have been the most extensively studied *via* DLS,<sup>[79]</sup> SANS,<sup>[73, 80]</sup> and shear-rheology<sup>[61, 64]</sup>. PEG is widely used for biomedical and biotechnological applications due to its anti-fouling properties, ease of synthesis, and ability to act as a blank slate for chemical modifications to control and direct cell functions. Early work has extensively elucidated the interactions between PEG/PEO and nanoclay.<sup>[11, 73, 79, 84]</sup> It is shown that PEG/PEO chains quickly desorb/adsorb onto nanoclay surface. These interactions can be modeled as a Newtonian fluid or Bingham Plastic, based on the concentrations of individual components within the solution.<sup>[73, 74]</sup> Nuclear magnetic resonance (NMR) relaxation data suggests that the hydrogens from the ethylene carbons in PEG/PEO can adsorb on the surface of nanoclay in lieu of water.<sup>[85]</sup> PEO adsorption onto nanoclay has also been demonstrated in tri-block copolymer systems containing alternating PEO and poly(propylene oxide) (PPO), commercially known as Pluronics or poloxamers).<sup>[80, 86]</sup> When PEG molecular weight is above 35 kDa, bridging of individual nanoclay via polymeric chains is observed.<sup>[61, 72]</sup> After stabilization due to bridging, the polymer-nanoclay solution remains stable, regardless of external ionic concentration, and exhibits yielding behavior only in the application of external stress. It is also observed that increasing the concentration of shorter chain PEG (3.4 kDa) also results in the formation of a stable gel when mixed with higher concentrations of nanoclay (> 4 wt.%) after 24 hours.<sup>[61, 72]</sup>

Solutions containing low amount of nanoclay (2 wt.%) can also form a weak gel over longer periods of time (months).<sup>[86]</sup> Due to the concentration-dependent properties of the nanoclay-polymer system, these interactions can be controlled to alter and modify the shear-thinning characteristics of the solution.<sup>[12]</sup> The addition of nanoclay to PEG/PEO hydrogels, reduces the flow behavior index and recovery time of the solutions, permitting *in situ* solidification upon injecting into the void.<sup>[87]</sup> It is observed that the recovery time of the system is dependent on the ratio of PEG to nanoclay, specifically on a balance between van der Waals attraction and electrostatic repulsion.<sup>[87]</sup> Similar to PEG/PEO, PNIPAM have also shown the effect of polymer adsorption and desorption on nanoclay surface.<sup>[83, 88]</sup>

Polymers with charged characteristics interact with nanoclay in significantly different ways.<sup>[89]</sup> Gelatin, a naturally derived protein from hydrolyzed collagen, assumes a random coil conformation in dilute solutions. Gelatin, containing positive and negative regions, can form strong electrostatic interactions with the oppositely charged regions of the nanoclay.<sup>[89, 90]</sup> Gelatin has polyampholyte properties, and therefore its surface charge is also dependent on pH of the solution;<sup>[91]</sup> for example, gelatin-A (isoelectric pH~9) and nanoclay exhibited preferential binding due to strong electrostatic interactions and results in a mildly turbid solution.<sup>[89]</sup> However, gelatin-B (isoelectric pH~5) exhibited a weaker interaction and resulted in the formation of smaller-sized complexes. The use of nanoclay within a gelatin hydrogel precursor solution has been used as a common shear-thinning hydrogel system for biomedical applications, flowing upon application of minimum shear forces and solidifying through rapid gelation after injecting into a void.<sup>[9]</sup>

Nanoclay-synthetic polymer interactions provide limited insight into interactions with biological polymers such as protein or DNA. These interactions are further complicated due to the ionic environment that proteins and DNA are typically found within (be it *in vivo* or *ex vivo*). For example, experiments to understand fundamental interactions between nanoclay and biopolymers are often performed in solution, with ions absent; however, under physiological conditions, the structure of exfoliated nanoclay is changed due to the inclusion of ions as previously discussed. In addition, studies that have used phosphate buffered saline (PBS) to exfoliate nanoclay met with limited success, as clay flocculates (or aggregates) out of solution. Therefore, it is imperative that the gelation/internal structure of nanoclay is strictly controlled for biomedical applications

Recent studies have shown that presence of ions induces the formation of nanoclay-polymer aggregates that significantly affect the rheological characteristics of nanocomposites (Fig. 5d).<sup>[92]</sup> Specifically, the effects of common salts such as sodium chloride (NaCl) and calcium chloride (CaCl<sub>2</sub>) on shear-thinning properties and the structural organization of nanoclay were considered. When nanoclay-gelatin hydrogels are prepared in water, a homogenous hydrogel is obtained, but when PBS is used instead of water nanoclay-polymer aggregates were formed. The formation of these aggregates results in ion-induced shrinkage of the diffuse double layer and eventually results in liquid-solid phase separation. This phase separation significantly alters the rheological and mechanical properties of gels due to changes in water content. Thus, it is important to control the fabrication process of nanoclay containing hydrogels to optimize physical characteristics.

## 6. Laponite® Nanoclay-based Biomaterials for Regenerative Engineering Applications

Regenerative engineering approaches include three major components - scaffolding, cells, and bioactive signals.<sup>[93]</sup> Nanoclays have been used to design a range of scaffolds including hydrogels, electrospun mats, and porous scaffolds. The direct interactions of nanoclay with cells have shown bioactive properties and can be used to control cell functions for tissue engineering applications. In addition, the high surface area and charged characteristics of nanoclay have been used to sequester and release various bioactive agents including small molecules drugs and large proteins. In this section, we will critically discuss each of these aspects and evaluate emerging and potential applications of nanoclay and nanoclay-based biomaterials in regenerative medicine.

### 6.1 Bone Tissue Engineering

Several studies have investigated bioactive characteristics of nanoclay, particularly its ability to induce osteogenic differentiation in pre-osteoblasts, hMSCs and human adipose derived stem cells (hASCs) in the absence of growth factors.<sup>[13, 54, 55]</sup> After establishing that nanoclay were not toxic to cells and did not damage the cell membrane, extensive differentiation assays were performed to determine the role of nanoclay in osteogenic differentiation of stem cells. Nanoclay exposure to hASCs led to a significant increase in alkaline phosphatase (ALP) activity, was also observed due to nanoclay treatment.<sup>[55]</sup> In addition, a significant increase in production of osteo-specific genes including 70-fold increase in Runt-related transcription factor 2 (RUNX2) on day 7, 9-fold increase in osteocalcin (OCN) on day 14, and 45-fold increase in osteopontin (OPN) on day 21 compared to controls (Fig. 6a).<sup>[55]</sup> In a similar study, a significant increase in mineralized extracellular matrix production was observed due to nanoclay treatment in the absence of growth factors (Fig. 6b).<sup>[54]</sup> Furthermore, collagen I production, which is important component of mineralized ECM, increased due to nanoclay treatment.<sup>[55]</sup> Although the exact mechanism of action has not been determined, both these studies suggest increased osteogenic differentiation could result from the dissociation of nanoclay into its individual ions ( $\text{Li}^+$ ,  $\text{Mg}^{2+}$ ,  $\text{Si}(\text{OH})_4$ ). Individually, these ions have shown to control several cellular processes, including the stimulation of osteogenesis.<sup>[44, 45, 49, 94]</sup> In a recent study, whole-transcriptome analysis revealed an upregulation of osteo-specific genes and signaling pathways in nanoclay-treated hMSCs.<sup>[13]</sup> The authors attributed these innate osteoinductive characteristics of nanoclay to both biophysical (physical shape, size and surface charge) and biochemical (ionic dissolution products) properties of the nanoparticle.<sup>[13]</sup>

While nanoclay in direct contact with cells was shown to stimulate osteogenesis, nanoclay-based scaffolds have also been investigated for bone tissue engineering.<sup>[95]</sup> Self-assembled gels are obtained by exfoliation of nanoclay and subjected to physiological conditions such as saline or serum solution. By drying these gels, nanoclay films are also obtained. Both nanoclay-based gel and films supported cell adhesion and proliferation (Fig. 6c).<sup>[95]</sup> When subjected to osteogenic conditions, seeded stem cells were induced towards osteogenic lineages. Osteogenic related genes such as collagen 1, RUNX2, and osteocalcin are significantly upregulated compared to control.<sup>[95]</sup>

In another study, scaffolds with smooth and porous morphology were obtained by sintering compacted nanoclay.<sup>[96]</sup> The sintered nanoclay scaffold supported high cytocompatibility and hemocompatibility, which were attributed to the hydrophilic characteristics of the scaffold. When subjected to simulated body fluid (SBF), the scaffolds promoted biomineralization.<sup>[96]</sup> Similar to previous findings, this study also showed that nanoclay induces osteogenic differentiation of stem cells in the absence of growth factors. Specifically, upregulation of ALP and mineralized matrix production were observed after nanoclay treatment. *In vivo* testing revealed minimal systemic toxicity of nanoclay, as evaluated through intraperitoneal injection of nanoclay extract. The treatment group of animals did not show any significant change in body temperature or body weight compared to the control group treated with saline solution, supporting the biocompatibility of nanoclay and extract. To evaluate the *in vivo* efficacy of nanoclay scaffolds for bone regeneration, rectangular bone defects were created in pig's front leg diaphysis. The results showed that defects treated with nanoclay scaffolds healed quickly within 24 weeks, while the control group showed limited bone healing (Fig. 6d).<sup>[96]</sup> These results strongly support that nanoclay based scaffolds can be used for bone regeneration *in vivo*.

Importantly, the bioactive characteristics of nanoclay are preserved after incorporation in synthetic polymer systems.<sup>[97]</sup> Apart from enhancing mechanical properties of the engineered scaffolds, nanoclay has been shown to facilitate cell adhesion and cell differentiation. For example, nanoclay-PEO nanocomposites showed increased cell adhesion and spreading, along with increased ALP and mineralized matrix production.<sup>[98]</sup> Similar studies have investigated the use of poly(glycerol sebacate) (PGS)- nanoclay for bone tissue engineering.<sup>[99]</sup> Both studies revealed enhanced osteogenic differentiation of pre-osteoblast cells on nanoclay-based scaffolds. Finally, electrospun scaffolds have been fabricated using poly(lactic glycolic acid) (PLGA) and nanoclay.<sup>[100]</sup> Uniform fibers were generated with the inclusion of nanoclay and increased protein adsorption and subsequent cell adhesion were observed.<sup>[101]</sup> Importantly, hMSCs seeded on the PLGA-nanoclay scaffolds successfully differentiated towards osteoblasts.

While synthetic polymers have shown successful regenerative properties, researchers have also been interested in exploring natural materials to mimic native ECM. One such material of interest is gelatin, as it is biodegradable and contains cell binding domains (RGD) for cell adhesion.<sup>[102]</sup> While biodegradation is ideal for tissue engineered scaffolds to allow for cellular remodeling, gelatin degrades too quickly (~2–4 weeks) and is fluidic at body temperature. To overcome these limitations, nanoclay have been incorporated with gelatin to form a mechanically stiff network.<sup>[89]</sup> Other studies have synthesized photocrosslinkable nanocomposites from gelatin methacryloyl (GelMA), and nanoclay.<sup>[103, 104]</sup> Incorporation of nanoclay in GelMA enhanced the mechanical properties, as well as increased osteogenic differentiation of seeded preosteoblasts<sup>[103]</sup> and encapsulated hMSCs<sup>[105]</sup>. These studies support the preservation of nanoclay bioactivity in both the 2D and 3D microenvironments.

In a recent study, injectable hydrogels have been fabricated by utilizing non-covalent interactions between DNA and nanoclay.<sup>[106]</sup> Specifically, utilizing DNA denaturation and rehybridization mechanisms, shear-thinning hydrogels were formed when mixed with nanoclay. These hydrogels could be injected within defect sites due to their rapid recovery

after cessation of stress. In addition, nanoclay based gels could be uniformly coated on the surface of a bone allograft to improve the osteointegration (Fig. 6e).<sup>[106]</sup> In this study, the nanoclay hydrogels were loaded with dexamethasone and evaluated for bone regeneration both *in vitro* and *in vivo*. The addition of nanoclay allowed for sustained release of dexamethasone and significantly increased ALP activity, production of osteo-related ECM including collagen I, and mineralized matrix. *In vivo* bone formation was demonstrated using a rat cranial defect model, and in the presence of nanoclay and released dexamethasone, new bone formation was observed. Overall, this study shows that the presence of nanoclay along with delivery of dexamethasone within the scaffolds were responsible for new bone formation.<sup>[106]</sup>

Other studies have investigated gelatin/carboxymethyl chitosan scaffolds with nanoclay for bone regeneration via *in vitro* and *in vivo* evaluation.<sup>[107]</sup> Similar to previous studies, increased osteogenic differentiation of seeded rat bone marrow-derived mesenchymal stem cells (rBMCs) was observed with the addition of 5 and 10 wt.% nanoclay. In addition, *in vivo* studies revealed increased bone regeneration in rat cranial defects treated with composite scaffolds.<sup>[108]</sup> Another natural material, alginate, along with methylcellulose and nanoclay have also been investigated for bone regeneration.<sup>[109]</sup> The material formulation shows great promise for future bone tissue regeneration strategies as it can achieve sustained delivery, good cytocompatibility and the necessary mechanical properties.

## 6.2 Cartilage Tissue Engineering

Cartilage tissue lacks vascularization and thus has a limited ability to regenerate.<sup>[110]</sup> In a recent study, the effect of nanoclay on chondrogenic differentiation of hMSCs was evaluated *via* transcriptomic analysis.<sup>[13]</sup> The gene tracks showed significant upregulation of chondro-related genes such as cartilage oligomeric matrix protein (COMP), and aggrecan (ACAN) (Fig. 7a).<sup>[13]</sup> COMP is one of the integral proteins of cartilage ECM and has been shown to interact with chondrocytes (cells present in cartilage tissues) through cell surface integrin receptors. In addition, significant production of chondrogenic ECM such as glycosaminoglycans (GAGs) and aggrecan was also observed after day 21. This study attributed the genetic effect of nanoclay to biophysical (cell-nanoparticle interactions) or biochemical (ionic dissolution of nanoclay) mechanisms, or a combination of both. Although these studies are newly published, there is strong potential support within this literature for the use of nanoclay for cartilage tissue engineering.

An earlier study demonstrated that treating hMSCs with nanoclay resulted in production of collagen type II, an important component of cartilage tissue.<sup>[55]</sup> The amount of collagen was directly dependent on nanoclay concentration and culture conditions (Fig. 7b).<sup>[55]</sup> When hMSCs were treated with different quantities of nanoclay and cultured in normal growth media, both collagen I and II were produced in equal amounts on day 7.<sup>[55]</sup> The amount of collagen II increased to >85% compared to collagen I on day 28. This strongly indicated that nanoclay might stimulate chondrogenic differentiation.<sup>[55]</sup>

Injectable nanoclay matrices for cell delivery have also been proposed for cartilage tissue engineering. The nature of cartilage presents difficulties for successful cell delivery. Specifically, within native cartilage, chondrocytes have a round shape morphology due to the

surrounding ECM which mostly consists of an interpenetrating network of glycosaminoglycans and proteoglycans that provide high mechanical strength.<sup>[111, 112]</sup> Polymers selected for cartilage tissue engineering aim to mimic ECM components such as hyaluronic acid, aggrecan, and collagen type II.<sup>[112, 113]</sup> Nanoclay have been incorporated in a variety of polymeric systems to obtain mechanically stiff hydrogels that mimic native cartilage, while maintaining a mesh size that facilitates cell migration. For example, polysaccharide-based hydrogels, specifically kappa-carrageenan (kCA), have been reinforced with nanoclay to obtain a shear-thinning precursor solution for cell delivery. After delivery, the solution can be crosslinked by utilizing monovalent or divalent cations to form mechanically stiff gels.<sup>[114, 115]</sup> High cell viability was maintained in these hydrogels after injection and, importantly, hMSCs maintained a round-shaped morphology that is critical to promote chondrogenic differentiation (Fig. 7c).<sup>[114]</sup> Injectable gels can be used for minimally invasive therapies to deliver hMSCs into the intraarticular space to promote production of cartilage-related ECM proteins.

In another study, nanoclay along with silylated hydroxypropylmethyl cellulose (Si-HPMC) was engineered for chondrocyte delivery.<sup>[116]</sup> An increase in nanoclay concentration resulted in rapid gelation and improved mechanical strength of crosslinked gels. However, the compressive moduli of crosslinked gels remained fairly low (~5kPa), compared to native cartilage. Encapsulated chondrocytes showed high viability and proliferation within nanoclay-loaded hydrogels. To investigate the ability of nanoclay-containing hydrogels to support *in vivo* chondrogenesis, subcutaneous implantation of gels loaded with chondrocytes was performed in nude mice. *In vivo* testing demonstrated high viability of encapsulated chondrocytes after implantation in nanoclay-containing gels. The encapsulated chondrocytes were able to produce cartilaginous ECM as demonstrated by Alcian blue and Masson trichrome staining (Fig. 7d).<sup>[117]</sup> The study also noted reduction in nodules (i.e. lacunae) surrounding the implanted chondrocytes, at a ~1% nanoclay concentration. Although the gels were injected in subcutaneous space, future studies could determine the efficacy of nanoclay-loaded gels after injection in intra-articular space.

Synthetic polymers have also been reinforced with nanoclay for cartilage tissue engineering.<sup>[118]</sup> For example, maleimide modified PEG was coupled with nanoclay to generate a resilient hydrogel with mechanical properties similar to native cartilage.<sup>[119]</sup> The PEG-maleimide/nanoclay gels showed high cytocompatibility when seeded with hMSCs for 14 days. Although the study proposes interesting materials with native-tissue like mechanical properties, it did not show chondrogenic differentiation of hMSCs. In a similar work, pluronic (PEO-PPO-PEO) was also combined with nanoclay to obtain mechanically stiff hydrogels for cartilage tissue engineering.<sup>[120]</sup> However, cellular investigations were lacking and the true potential of hydrogels for cartilage regeneration was not demonstrated. In another study, pluronic/nanoclay was reinforced with chitosan and keratin.<sup>[121]</sup> Chitosan, a polysaccharide, has similar structure compared to glycosaminoglycans. Alternatively, keratin contains RGD domains to facilitate cell adhesion and mechanically reinforced the network upon covalent crosslinking due to the addition of genipin. Hydrogels containing nanoclay displayed high cell viability up to 14 days and stimulated differentiation of encapsulated cells.



Despite various studies showing the promise of nanoclay in designing scaffolds for cartilage tissue engineering, more extensive *in vitro* and *in vivo* analyses are needed. Specifically, the effect of nanoclay on chondrogenic differentiation of hMSCs or production of cartilage-specific ECM by chondrocytes are not well understood or characterized.

### 6.3 Osteochondral Tissue Engineering

While several strategies have been developed for bone and cartilage tissue regeneration, another important topic in tissue repair is engineering tissue interfaces such as the bone-cartilage interface. In the case of osteoarthritis, not only is the bone damaged but more importantly, so is the underlying cartilage. In addition to generating strategies to repair bone tissue, there is a need to regenerate this bone-cartilage tissue interface.<sup>[122]</sup> Nanoclays are unique in that they have been shown to stimulate both osteogenesis and chondrogenesis in hMSCs.<sup>[13]</sup> In a combinatorial study, nanoclay was incorporated into two natural polymer scaffolds and a gradient nanocomposite was fabricated with the potential to mimic the unique properties of both bone and cartilage.<sup>[123]</sup> Specifically, nanoclay-GelMA was utilized for the bone region and nanoclay-methacrylated kappa-carrageenan (MkCA) was used for the cartilage region. While osteogenic and chondrogenic differentiation were not assessed in this study, the scaffold demonstrated varied mechanical properties and cellular morphology across the gradient, showing promise for future regeneration strategies.

### 6.4 Cell Adhesion and Cell Sheet Engineering

For tissue regenerative approaches, protein adsorption is desirable to promote cell adhesion and integration with native tissue. Various approaches were investigated for controlled protein adsorption via use of RGD peptide or surface patterning to promote cell-matrix interactions.<sup>[124]</sup> While these techniques have been successful they may also require more extensive scaffold preparation. As a simpler alternative, more recent studies have investigated the incorporation of nanoclay into polymeric biomaterials to support cell adhesion.<sup>[98]</sup> Overall, the cell adhesion on clay-based biomaterials can depend on three major factors: (a) increase in mechanical properties of scaffolds due to ability of nanoclay to reinforce the network, (b) charge characteristics of nanoclay to facilitate adsorption of serum protein, and/or (c) presence of minerals that support integrin binding.

Studies have shown that cell adhesion and spreading increased as a function of nanoclay concentration in poly(ethylene oxide) (PEO) scaffolds.<sup>[98, 125]</sup> PEO is a non-fouling polymer used as a “blank slate” for chemical modifications to control and direct cell functions. Nanocomposite containing 60% PEO - 40% nanoclay showed minimal cell adhesion (Fig. 8a).<sup>[98]</sup> Some cells that were able to adhere on the surface exhibited round-shaped morphology, indicating minimal anchoring points present on the surface. As the nanoclay concentration increased, an increase in cell adhesion and spreading was observed. Importantly, the spread-out cell morphology on scaffolds containing 30% PEO - 70% nanoclay closely resembled that of the tissue culture polystyrene (TCPS) control.<sup>[98, 126]</sup> It was hypothesized that cell adhesion might be attributed to adsorption of serum protein on charged nanoclay surfaces. To verify this, cell adhesion on nanocomposite surface was evaluated in the presence and absence of serum proteins. The results revealed cell adhesion on nanoclay-rich surfaces even in the absence of serum protein. However, cell spreading was

highly dependent on protein adsorption in the presence of nanoclay. It is expected that minerals present on nanoclay surface could facilitate cell adhesion. For example, the divalent cation ( $Mg^{2+}$ ) was shown to mediate cell adhesion through increased integrin interactions.<sup>[94]</sup> Furthermore, the charged nature of nanoclay could facilitate protein aggregation or clustering due to electrostatic interactions with cell membrane proteins. Although nanoclay-mediated cell adhesion has been established, the role of divalent cations and/or clustering of cell membrane proteins has yet to be investigated.

Similar to PEO, poly(ethylene glycol) (PEG)-based hydrogels have also been investigated after nanoclay inclusion for increased protein adsorption as PEG alone is also bio-inert.<sup>[127, 128]</sup> These studies showed that addition of nanoclay to polymer resulted in an increase in mechanical stiffness. While hMSCs were also encapsulated within the three-dimensional matrix, cell spreading within the hydrogel was not monitored. Importantly, this study evaluated the interactions of nanoclay with lower molecular weight PEG (3.4–10 kDa) and demonstrated that strong networks were still formed that allow for cell adhesion.<sup>[127]</sup> In a similar study, nanoclays were incorporated in high molecular weight PEG (34 kDa) and increased cellular adhesion and spreading were observed with the addition of 5% nanoclay in 20% PEG. However, contrary to previous studies, the compressive moduli remained similar with increasing nanoclay content. The researchers attribute the steady mechanical properties to the nanoclay inclusion, which should increase moduli, being balanced by the rearrangement of the physical crosslinks between PEG and nanoclay, which would decrease mechanical stiffness.<sup>[129]</sup> This study delineated the mechanical effect on cell adhesion and demonstrated that nanoclays are mainly responsible for enhanced cell adhesion and spreading.

Another synthetic polymer with low protein adsorption that has incorporated nanoclay is poly(2-methoxyethyl acrylate) (PMEA). While PMEA has been included in various copolymer systems, in isolation the polymer is weak and cannot form a stand-alone film. However, the inclusion of nanoclay in PMEA results in increased mechanical strength and stability.<sup>[82]</sup> In one study, PMEA-nanoclay nanocomposite was seeded with various cell types (normal human dermal fibroblasts, normal human umbilical vein endothelial cells, and primary normal bovine aortic endothelial cells) to evaluate cell adhesion.<sup>[130, 131]</sup> Cell adhesion on nanocomposites with 15% nanoclay revealed no significant difference between the nanocomposite and the control TCPS for all four cell types. This study supports the fact that nanoclay actively influences cell adhesion and spreading.

In addition, poly(*N*-isopropylacrylamide) (PNIPAM) has been investigated in conjunction with nanoclay for cell sheet engineering (Fig. 8b).<sup>[131, 132]</sup> Similar to the PMEA-nanoclay composite, this study also indicated support of cell adhesion and proliferation on PNIPAM-nanoclay composites compared to a TCPS control. It was hypothesized that the balance in hydrophobicity provided by the PNIPAM backbone against the hydrophilic nanoclay could provide a suitable surface for protein adsorption and cell adhesion. Specifically, it was mentioned that the prevalence of surface charge provided by nanoclay enables protein adhesion to the hydrogel surface and subsequent binding to cell receptors. By utilizing the lower critical solution temperature (LCST) of PNIPAM ( $\sim 32$  °C), a confluent cell sheet was harvested from the nanocomposite surface for cell sheet engineering.<sup>[133]</sup> These cell sheets

provide initial cell organization that can be utilized for further engineering applications into scaffold-free systems.

### 6.5 Tissue-adhesive, Surgical Glue and Wound Healing Patch

Nanoclays provide a platform for enhanced polymer interactions *via* hydrogen bonding and the inherently charged nature of the nanoclay. This attribute has merit in specific biomedical applications where mechanical integrity and adhesion are imperative for device success. Specifically, applications related to wound closure of non-flat geometries require dry/wet adhesives as an alternative method of sealing tissues. Earlier studies have shown that addition of nanoclay to PEG not only improves shear-thinning properties required for minimally invasive therapy, but also impart adhesive characteristics to dry surfaces such as skin.<sup>[129]</sup> However, addition of nanoclay was not sufficient for wet tissue adhesion. To improve the tissue adhesion, nanoclay have been combined with dopamine-modified PEG.<sup>[59, 134]</sup> Dopamine is a catecholic moiety that has shown to have strong interfacial binding and intermolecular cross-linking ability. To obtain a wet sealant, dopamine-modified multi-armed PEG (PEG-D) is mixed with nanoclay to form a reversible gel. The addition of dopamine improves the mechanical properties and recoverability of hydrogels.<sup>[59, 134]</sup> Nanoclay-loaded solutions demonstrated enhanced cellular infiltration compared to control (polymer only) and also exhibited a minimal immune response (Fig. 8c).<sup>[134]</sup> Specifically, solutions can be injected to fill complex architectures and exhibit strong adhesiveness to both dry and wet surfaces.<sup>[59]</sup> The wet adhesion properties can be modulated by controlling nanoclay concentration.<sup>[59, 134]</sup> These properties allow this fit-to-shape sealant to be used as an injectable bandage.

Wound healing depends on numerous factors, including the biodegradability of the scaffolding, injectability, prevention of bio-fouling, pH-change, cell adhesion onto the scaffolding, and recruitment of the immune response *via* cytokines. Chronic wounds are notoriously slow to heal, as confirmed in a study that verified the poor proliferation abilities of fibroblasts within a chronic wound.<sup>[135]</sup> Additionally, it has been shown that wound sites are typically acidic, an additional hurdle for an already complicated problem.<sup>[136]</sup> The acidic environment of the wound bed has the potential to cause dissociation of nanoclay into its individual ions ( $\text{Li}^+$ ,  $\text{Mg}^{2+}$ ,  $\text{Si}(\text{OH})_4$ ). This dissociation has the ability to release magnesium into a wound site, which has shown to improve the inflammatory response as well as stimulate cellular proliferation and healing.<sup>[137]</sup> The exact regulatory mechanisms of this phenomenon are currently unknown, but there is a correlation between magnesium release and wound healing rate. Therefore, based on the biophysical aspects of nanoclay, this approach has potential wound healing applications.

Nanoclay can stimulate wound healing through the generation of ROS, which have been correlated to upregulation of the vascular endothelial growth factor (VEGF) pathway as well as increased cellular proliferation and vascularization within the wound site.<sup>[54, 138]</sup> ROS also have the ability to attract inflammatory cells, a necessary factor in wound healing. Cellular response is important to the healing process, so harnessing relevant cytokines such as VEGF and the recruitment of inflammatory cells is imperative for the chronic wound treatment. One study reported the synthesis of nanoclay functionalized with amino acids for

wound healing applications<sup>[139]</sup> wherein the researchers observed that nanoclay functionalized with arginine generated significantly more ROS than a nanoclay alone, and also stimulated fibroblast proliferation. This observation was validated by performing a scratch test assay to show that nanoclay/arginine facilitated wound-closure *in vitro* and could be used for wound healing applications.<sup>[139]</sup>

In another study, pH responsive wound dressing was designed to release encapsulated drugs via external stimuli.<sup>[140]</sup> Specifically, the design was composed of an electronic driver, microelectrodes fabricated on a flexible substrate, and PEG/nanoclay loaded with chitosan particles (ChPs). The application of external voltage results in local pH change that triggers release of encapsulated drugs in chitosan particles. The role of nanoclay is to enhance drug retention and improve physiochemical properties of PEG hydrogels. This study showed that application of external voltage does not influence wound healing rate,<sup>[141]</sup> and highlights the use of nanoclay in designing smart bandages that respond to wound microenvironment such as change in pH.

Wound sites are typically irregular in shape, therefore it is necessary for the system to be injectable and preferably shear-thinning.<sup>[142]</sup> In addition, a wound dressing must be adhesive and provide a moisture-balanced environment to promote cell migration and proliferation.<sup>[143]</sup> The addition of nanoclay within a PVA-Alginate hydrogel provided increased mechanical integrity as well as decreased swelling and degradation rates.<sup>[144]</sup> These material characteristics are useful in wound healing, as lower swelling facilitates cell migration and proliferation, and slower degradation provides time for tissue remodeling.

In a recent study, nanoclay-based nanocomposite hydrogels have been investigated as chronic wound dressings for patients suffering from diabetes mellitus.<sup>[145]</sup> Nanoclay was added to improve the mechanical properties of hydrogel networks. The study showed that nanoclay improved the mechanical stiffness and elastomeric characteristics of the hydrogels. Complete closure of normal and diabetic wounds with the nanoclay-based wound dressing was observed after 10 and 12 days respectively (Fig. 8d).<sup>[145]</sup> Additionally, complete re-epithelialization and formation of new connective tissues was also observed when a nanoclay-based dressing was used.<sup>[145]</sup>

## 6.6 Hemostat and Embolization

Nanoclay possess multiple properties that are directly applicable to hemostasis and endovascular embolization applications.<sup>[146]</sup> The dual charged surface of nanoclay can attract proteins present in blood and activate the clotting cascade.<sup>[147]</sup> When nanoclays are mixed with polymeric solution, shear-thinning hydrogels are obtained, which could be used as an injectable bandage for difficult to reach areas such as internal injuries. For example, nanoclay can be combined with gelatin<sup>[147, 148]</sup> or kappa-carrageen<sup>[149]</sup> to obtain injectable hemostats (Fig. 9a)<sup>[147]</sup>. The shear-thinning characteristics of these composite gels permits minimally invasive procedures, eliminating the need for surgical implantation. The incorporation of nanoclay in polymer has shown to reduce the clotting time by 77%, which is similar to the gold standard heparin (Fig. 9b). Blood clotting was observed to be dependent on nanoclay concentration, indicating its significant role in the coagulation cascade.

Although the exact mechanism of clotting by nanoclay is unknown, it is hypothesized to be attributed to the adhesion and activation of platelets (Fig. 9c).<sup>[150]</sup> A recent study observed that, similar to serum protein, blood components such as platelets and red blood cells (RBCs) readily attach to nanoclay-based hydrogels. The high negative charge of the nanoclay surface may facilitate these interactions. Earlier studies have shown that a negatively charged surface can potentially trigger intrinsic coagulation pathways through activation of Hageman factor (FXII) and platelets.<sup>[151]</sup> A rapidly injectable hydrogel with the ability to accelerate clot formation has the potential to prevent excessive blood loss and fatality. Shear-thinning characteristics of nanoclay-based solutions can be used as an injectable bandage to prevent excessive bleeding in limited resource settings.<sup>[150]</sup>

Along a similar direction, nanoclay-gelatin based injectable hydrogels have been investigated for use in endovascular embolization.<sup>[148]</sup> Similar to previously reported findings, researchers observed that the shear-thinning properties of these nanoclay hydrogel composites facilitated the injection of the gel through clinical catheters and needles. Additionally, the hemostatic activity of nanoclay-based gels is comparable to metallic coils, currently used as the clinical gold standard. Due to elastomeric characteristics, these gels were able to withstand physiological pressures. Interestingly, nanoclay-based gels did not rely on the intrinsic ability of blood to form clots and therefore may be used in patients receiving anticoagulation therapy or those with coagulopathy. Researchers also demonstrated the ability of injectable nanoclay-based gel embolization in the forelimb venous vasculature of pigs. All the pigs in the *in vivo* study survived and no evidence of pulmonary embolism was observed up to 24 days. The histologic and immunohistochemical assessment of the embolized veins indicated the presence of myeloperoxidase (MPO)-positive cells and macrophages (CD68), suggesting degradation of the nanoclay-based gels. Based on these data, nanoclay-gelatin based hydrogels can potentially address the clinical need to develop a less invasive injectable endovascular embolization method.

## 6.7 Immunomodulation and 3D Organoid

Previous studies have suggested a linkage between the individual ions ( $\text{Li}^+$ ,  $\text{Mg}^{2+}$ ,  $\text{Si}(\text{OH})_4$ ) within nanoclay and immunomodulation. Specifically, lithium has been shown to enhance mitogen response, inhibit suppressor T cells, and stimulate B lymphocyte immunoglobulin IgG and IgM production.<sup>[152]</sup> In addition, magnesium has shown to play a role in the immune system and have potential immunomodulatory effects.<sup>[153]</sup> One study demonstrated that titanium doped with increasing amounts of magnesium increased M2 polarization, and subsequently enhanced tissue healing.<sup>[154]</sup> Sodium silicate containing materials, specifically Baradon®, have also demonstrated immune stimulatory effects in both equine and porcine lymphocytes.<sup>[155]</sup> In another study, pure sodium metasilicate exhibits immune stimulatory effects as well as activates mitochondria activity. It is postulated that immune stimulation observed in these studies involving sodium silicate results from the release of orthosilicic acid.<sup>[156]</sup> Based on these observations, it is expected that nanoclays have immunomodulatory properties.

In a recent study, osteoimmunomodulatory properties of nanoclay have been investigated for bone regeneration.<sup>[157]</sup> This is the first study to show that nanoclay can induce a phenotypic

switch in macrophages in the presence of rat bone marrow mesenchymal stem cells (rBMSC) to promote bone formation *in vitro* and *in vivo* (Fig. 10a).<sup>[157]</sup> As the nanoclay concentration was increased from 12.5 µg/mL to 100 µg/mL, a decrease in anti-inflammatory factors (IL-10, IL-1ra, and Arg-1) and an increase in pro-inflammatory factors (TNF-α, IFN-γ, IL-6, and IL-1β) were observed in macrophages. Specifically, pro-inflammatory factors were significantly downregulated and anti-inflammatory factors were upregulated in the nanoclay/rBMSC/macrophage co-culture group in comparison to the nanoclay/macrophage group. Immunohistochemical staining of M1 and M2 markers were performed to investigate the role of macrophage polarization on bone regeneration. In the nanoclay group, elevated CCR-7 and CD11c (M1)-positive stained cells were found in comparison to the nanoclay/rBMSC group. However, a significant increase in CD163 (M2)-positive cells was observed in the nanoclay/rBMSC group, compared to the nanoclay group.<sup>[157]</sup> Overall, this study showed that nanoclay in combination with bone marrow stem cells can display osteoimmunomodulatory properties that could be leveraged for regenerative medicine applications.

In another study, nanoclay have shown to play an important role in culturing primary immune cells to obtain immune organoids (Fig. 10b).<sup>[158, 159]</sup> *Ex vivo*, 3D immune organoids are expected to help understand the biological function of the immune system in real-time and potentially accelerate the translation of immunotherapies. In 2D culture, B cells can be activated using antibodies (anti-CD40 or anti-Ig) through stimulation of CD40L and IL-4, which is the current gold standard to understand the kinetics of germinal center-like reactions or antibody class switching.<sup>[158]</sup> However, this approach has poor cell yield and limited cell survival. Nanoclay-based platforms have been developed to engineer B cell follicles *ex vivo* by providing structural and signaling cues similar to the lymphoid microenvironment in order to promote germinal center-like reactions. Through the optimization of the microstructure of nanoclay-based platforms, 3D immune organoids were obtained by encapsulating primary naïve B cells co-cultured with stromal cells. This study established that 3D immune organoids resulted in a 100-fold increase in primary naïve B cells and promoted rapid differentiation to the germinal center phenotype with robust antibody class switching.<sup>[158]</sup> In the absence of nanoclay, proliferation of primary naïve B cells as well as differentiation to the germinal center phenotype were not observed. Although the exact role of nanoclay is not well established, these studies indicate that nanoclay play a crucial role in the induction of a germinal center phenotype in naïve B cells cultured in 3D organoids.<sup>[158, 160]</sup> Overall, this study showed that nanoclay-based biomaterials can be designed for antibody-based immunotherapy for treating various pathological conditions, including autoimmune diseases, infections, and cancers.

## 7. Laponite® Nanoclay for Sustained Delivery of Therapeutic Drugs and Proteins

The unique physiochemical properties of nanoclay that make these nanoparticles an excellent gelling agent and allow for strong interactions with polymers also make it a viable option for therapeutic delivery. A range of studies have investigated the use of nanoclay as a therapeutic delivery vehicle.<sup>[161, 162]</sup> The dual charge characteristic of nanoclay permits for

secondary interactions with delivery molecules. Specifically, neutral biomolecules can bind to nanoclay *via* hydrogen bonding, whereas cationic or bio-functional therapeutics can bind *via* an ionic exchange.<sup>[163]</sup> The intercalation of these molecules into the nanoclay layers occurs in a manner similar to that of polymers. The interaction of the biomolecules also depends on the local pH of the solution, with the optimal pH for intercalation depending on the properties of the molecule of interest. In the following sections, we review nanoclay as a delivery vehicle for both small (cancer drug, steroids, amino acids, antibiotics) and large (proteins) therapeutic agents.

### 7.1 Small Molecules: Steroids, Cancer drugs, and Antibiotics

Nanoclay-based drug delivery systems have multiple desirable features such as sustained release, high loading capacity, preserved bioactivity, and enhanced aqueous solubility of drugs.<sup>[164]</sup> Utilizing the interlayer spacing of the nanoclay, drugs can be incorporated *via* ionic exchange.<sup>[165]</sup> A range of small molecules including steroids, cancer therapeutics and antibiotics can be sequestered for prolonged release (Fig. 11a). Doxorubicin has previously been sequestered on the nanoclay surface with high loading efficiency and demonstrated enhanced cellular permeation compared to free doxorubicin (Fig. 11b).<sup>[166]</sup> Importantly, sustained and prolonged release of doxorubicin was observed. At the lower pH (5.4), doxorubicin release was almost two-fold higher than at physiological pH, suggesting this delivery system would be ideal for delivery to malignant tumors,<sup>[162]</sup> as the external pH environment is more acidic than healthy tissue. To further improve the cellular uptake of doxorubicin loaded nanoclay, a biocompatible polymer, alginate, has been used to coat nanoclay/doxorubicin complexes.<sup>[167]</sup> Similar to previously published reports, the nanoclay/doxorubicin/alginate system showed high encapsulation efficiency (~80%), pH-responsiveness, and sustained release profile.

The process of intercalating drug molecules within the interlayer space of nanoclay has also been studied for a variety of different small molecules, including dexamethasone,<sup>[168]</sup> tetracycline,<sup>[169]</sup> and itraconazole<sup>[170]</sup>. For example, nanoclay-based hydrogels have shown to entrap glucocorticoid such as dexamethasone to induce bone regeneration in craniofacial defect.<sup>[106]</sup> They showed that nanoclay can sequester dexamethasone and preserve the bioactivity to induce new bone formation (Fig. 11c).<sup>[106]</sup> Similar to studies with doxorubicin, the release rate of the intercalated drugs can be modulated by external stimuli such as pH. This property has been exploited to generate pH sensitive delivery systems with high drug loading efficiency. Some pH sensitive delivery systems incorporate the nanoclay-drug assembly within a polymeric coating to prevent burst release. Furthermore, in comparison to other nano-delivery systems that may persist in the body or degrade into toxic by-products, nanoclay are composed of complex polyions and degrade into non-toxic ionic products that are easily absorbed.<sup>[9]</sup>

Another delivery approach that uses nanoclay is the development of drug releasing hydrogels, in which effective delivery of both hydrophilic and hydrophobic drug molecules can be achieved.<sup>[8]</sup> For example, antibiotics have been incorporated into these nanocomposite systems for sustained release. In one study, mafenide, an antibiotic used for burn wounds, was incorporated into a nanoclay-Alginate composite.<sup>[137]</sup> In media, 90%

burst release of drug was observed within the first few hours, supporting cation exchange as the cations in the media replaced the intercalated mafenide. In another study, nanoclay was included in a multi-block co-polymer (pluronic) to deliver lysozyme. Nanoclay inclusion prolonged the release time to ~40 days, whereas the pluronic alone released lysozyme quickly within few days. This sustained release suggested strong interaction between the lysozyme and nanoclay. The incorporation of higher concentrations of nanoclay into hydrogels results in formation of an injectable system.<sup>[171]</sup> The combination of these two approaches allows the fabrication of injectable nano-delivery systems with pH triggered spatial release of the drug.

Finally, a more recent development is the surface modification of nanoclay to facilitate binding of multiple molecules on the surface of the nanoclay. This process is performed by modifying the surface hydroxyl groups by treatment with compounds, such as 3-aminopropyltrimethoxysilane (APTES), to convert the hydroxyl groups to amines. This is generally followed by conjugation of the target molecule to the amines *via* NHS-EDC chemistry. When compared to the standard intercalation techniques, this process limits the pH sensitivity of the nanoclay-drug complex, while simultaneously increasing the stability of the complex and preventing off target release of the drug.<sup>[162]</sup>

## 7.2 Macromolecules - Proteins

Nanoclay have also been investigated for therapeutic delivery of multiple growth factors.<sup>[172]</sup> Growth factors are often incorporated in synthetic biomaterials to facilitate or direct cell fate; however, complications have arisen with the use of high dosages.<sup>[173]</sup> As an alternative, nanoclay has been investigated to prolong delivery of therapeutic growth factors. A range of proteins including vascular endothelial growth factor (VEGF), bone morphogenetic proteins 2 (BMP2), Platelet-derived growth factor (PDGF), Fibroblast growth factor (FGF), and stem cell secretome are sequestered for prolong delivery using nanoclay-based biomaterials (Fig. 12a). Utilizing the strong interactions between nanoclay, several studies have developed nanoclay gels for delivery of these growth factors.<sup>[174, 175]</sup> Specifically, extensive investigations into the clay gel formation and ability to release model proteins (albumin and lysozyme) were performed and compared to alginate gel controls.<sup>[174]</sup> The nanoclay gels not only prolonged the protein release rate compared to alginate gels, but also increased protein adsorption or localization.

By sequestering BMP2 within nanoclay gel, it is possible to produce successful induction of osteogenesis in cells.<sup>[96, 174, 175]</sup> BMP2 was either encapsulated within or localized on nanoclay gels and cells were seeded on the gels to assess osteogenic differentiation.<sup>[175]</sup> Interestingly, cells seeded on gels with encapsulated BMP2 exhibited less differentiation than those seeded on gels with exogenous, localized BMP2.<sup>[175]</sup> *In vivo* studies revealed an increase in bone tissue formation when the clay-gel loaded with BMP2 was functionalized to a trabecular bone graft (TBG) (Fig. 12b).<sup>[175]</sup> This study highlights the idea that sustained and prolong delivery of BMP2 can reduce effective concentration of protein by 10–100 folds which is important to overcome clinical problems related to supraphysiological doses of BMP2. While the study does not necessarily demonstrate sustained delivery of the



therapeutic, it does explore the potential for nanoclay to sequester and localize therapeutics for direct delivery to cells.

In a similar study, when human umbilical vein endothelial cells (HUVECs) were seeded on the gel surface (loaded with VEGF), tubular formation was observed comparable to that of HUVECs treated with exogenous growth factor.<sup>[174]</sup> When collagen loaded with nanoclay/VEGF was implanted, an extensive network of new blood vessels was formed (Fig. 12c).<sup>[174]</sup> Both vessel volume and number were increased due to sequestering of VEGF on nanoclay. This study clearly indicates that nanoclay can sequester and preserve growth factor activity *in vivo* to direct tissue formation.

In a recent study, transforming growth factor beta 3 (TGF- $\beta_3$ ) was electrostatically bound to nanoclay to stimulate chondrogenic differentiation of hMSC spheroid (Fig. 12d).<sup>[176]</sup> After only 7 days of culture, hMSCs treated with nanoclay/TGF- $\beta_3$  exhibited increased expression of cartilage oligomeric matrix protein (COMP) compared to the control treated exogenous TGF- $\beta_3$ . Matrix synthesis was also monitored after 21 days and an increase in sulfated glycosaminoglycan (GAGs) production was observed in the hMSC spheroid culture treated with the co-delivery of nanoclay/TFG- $\beta_3$ . Importantly, this TGF- $\beta_3$  delivered via nanoclay was at a 10-fold lower concentration than the TGF- $\beta_3$  exogenously delivered. In addition, this study not only highlighted sustained delivery of therapeutic growth factors but also demonstrated the potential of nanoclay in the presence of lower dosages of growth factor to augment cell differentiation.

To assess the nanoclay gel's potential, both VEGF and BMP2 were exposed to the gel and the system was implanted in a murine bone defect.<sup>[175]</sup> While the combined effect was not extensively discussed, the potential of this system holds promise for future therapeutic delivery. Other recent studies have utilized the ability of nanoclay to sequester and prolong the release of multiple growth factors. Specifically, they loaded a range of pro-angiogenic growth factors including VEGF, FGF, PDGF on nanoclay surface.<sup>[177]</sup> The bioactivity of sequestered growth factor is demonstrated by 3D invasion assay, where surface seeded HUVECs migrate within growth factor loaded gels.

The stem cell secretome is cocktail of multiple growth factors, and has been sequestered using nanoclay to direct cell functions.<sup>[178]</sup> For example, to regenerate the cardiac tissue after myocardia infraction, nanoclay loaded with stem cell secretome was evaluated to promote angiogenesis.<sup>[179]</sup> An injectable hydrogel was fabricated from GelMA and nanoclay to deliver secretome media to the site of myocardial infarction.<sup>[180]</sup> The results revealed that growth factors, such as VEGF and fibroblast growth factor-2 (FGF2), could be successfully delivered utilizing the nanoclay-GelMA hydrogels. This is important because the release of the stem cell secretome was prolonged and could then be delivered directly to the wound site. *In vivo* studies further provided strong evidence to support the potential of nanoclay-based biomaterials as an alternative treatment option for myocardial infarction.<sup>[179]</sup> This controlled release mechanism, due to nanoclay addition, was responsible for regeneration of damaged cardiac tissue.

Nanoclays have also been used as vaccine adjuvants in stimulating effective immune responses.<sup>[181]</sup> Macrophages are primary antigen presenting cells (APCs) and play an important role during vaccine stimulation by facilitating cellular and humoral responses. Due to the charged nature of nanoclay, multiple vaccine adjuvants can be loaded on nanoclay surfaces (Fig. 12e).<sup>[182]</sup> Nanoclays facilitate uptake of the antigen by APCs as well as inducing strong antibody and cell-mediated immune responses compared to commercial adjuvants.<sup>[183]</sup> In addition, nanoclays are more efficient compared to commercially available adjuvants - QuilA and Alum.<sup>[183]</sup> Nanoclay treatment also induce macrophage maturation as evidenced by expression of co-stimulatory cytokines. Through the expression of co-stimulatory molecules and major histocompatibility complex (MHC) antigens, macrophages have ability to prime naive T cells. The study showed that use of nanoclay results in maintenance of strong immune responses for at least four months and no significant change in histopathology of the animal organs was observed.<sup>[184]</sup> Overall, these studies showed that nanoclay can be used to accomplish high and safe immune response compared to other commercially available adjuvants.

## 8. Laponite® Nanoclay for Additive Manufacturing

Additive manufacturing has demonstrated boundless potential as a versatile method to fabricate functional structures for applications in various fields, including electronics<sup>[185]</sup>, medical implants<sup>[186]</sup>, culinary, and civil applications. With the rapid expansion of this technology into the biomedical field, extrusion-based 3D printing has become a common printing platform to fabricate complex, anatomically accurate geometries from precise deposition of materials, cells, and/or bioactive molecules.<sup>[187]</sup> Extrusion-based modalities provide a means to fabricate geometries with specific macro- and micro-scale geometries, mimicking the complexity associated with tissues and allowing for cellular and nutrient transport.<sup>[188]</sup> Extrusion-based 3D printing has been conducted through the development and manipulation of diverse materials, or inks, such as ceramics, metals, thermoplastics, hydrogels, and/or their combinations. Although these materials contain extremely diverse properties, they can all be extruded due to common rheological properties, specifically viscoelasticity, shear-thinning, and yield-stress to flow.<sup>[186, 189]</sup> These properties dictate a material's printing fidelity and ease of manipulation during the extrusion process. In this section, we will discuss different nanoclay-based approaches (Fig. 13a) that have been investigated for 3D printing applications, including bioprinting, sacrificial support baths, and 4D Printing.

### 8.1 Nanoclay-based Inks for 3D Printing

Nanoclays have been added to polymeric systems to modulate and manipulate their physical and chemical properties, including flow behavior, stiffness, swelling, degradation, and function of the constructs being produced. The addition of nanoclay to polymers may generate an internal structure within the solution, permitting shear-thinning properties and increased recoverability while not compromising the overall composite's molecular structure. Nanoclay-based hydrogels are a useful material for 3D printing, due to their extrudability and rapid recovery. For example, PEG-alginate's precursor solutions are often too fluidic for the construction of scaffolds with high fidelity. The addition of nanoclay to

polymeric solution (PEG-alginate) allowed for the formation of elastomeric 3D printed structures that could recapitulate the properties of soft tissue.<sup>[190]</sup> The incorporation of nanoclay into the hydrogel matrix did not impede the matrix's gelling mechanism (e.g. photo-crosslinking, physical entanglements). Instead, the reversible molecular structure, provided by the nanoclay, elicited strong shear-thinning profiles and rapid recoverability for high fidelity extrusion of the bioink. These printed structures supported high cell viability and support long-term culture.

Other studies have also shown that the incorporation of nanoclay into hydrogel-precursor solutions provides a tool to control and alter the rheological parameters of these solutions, producing an ink that can be extruded into complex geometries.<sup>[127]</sup> When nanoclay is introduced at relatively high concentrations (>2 wt.%), a “*house-of-cards*” structure is formed through electrostatic interactions between the negative surface and positive edge.<sup>[69, 191]</sup> This structure increases the low-shear viscosity of the hydrogel solution, while enabling full recovery upon removal of high shear forces.<sup>[86]</sup> For example, hydrogel precursor solutions, such as gelatin methacrylate or poly(ethylene glycol) diacrylate exhibit Newtonian (water-like) flow profiles, meaning the viscosity of the material remains constant as the shear stress increases. Although these materials can flow on their own, the stress needed for extrusion of these inks are negligible and therefore there is a lack of control over the amount of material being extruded. However, upon the incorporation of nanoclay in the hydrogel precursor solution, the “*house-of-cards*” structure increases the materials low-shear viscosity while the viscosity decreases upon the exposure to higher shear stresses.<sup>[86]</sup> This allows for increased control over the stress necessary for the printer for flow in addition to the extruded volume.

The use of nanoclay to significantly alter the flow properties of bioinks has been growing in popularity. In one recent example, nanoclays were incorporated into a kappa-carrageenan bioink to improve its printability.<sup>[192]</sup> A range of concentrations were explored by combining un-extrudable kappa carrageenan bioinks with 3–6% nanoclay. Overall, the incorporation of nanoclay enabled the extrusion of the filament into smooth, consistent geometries, improving the overall printability of the kappa carrageenan. This property was attributed to the ability of nanoclay to reversibly interact with the polymer, preventing premature gelation by interfering with kappa carrageenan.<sup>[192]</sup>

In addition to improving printability, nanoclay can also imbue bioinks with additional functionalities. In a recent paper, not only was the printability of an alginate/methylcellulose based bioink improved by the addition of nanoclay, but also its ability to enable sustained protein release from the printed structures.<sup>[109]</sup> Bovine serum albumin (BSA) and VEGF were both used as model proteins to establish the sustained drug delivery enabled by the nanoclay. It was found that nanoclay-containing bioinks released model proteins in a sustained manner, which may lead to prolong delivery of bioactive substances to cells in and around printed structures, improving control over cell behavior.<sup>[109]</sup>

Even without binding bioactive substances, nanoclays have also been shown to directly affect cell behavior within printed structures. When nanoclays were incorporated into a PEGDA hydrogel co-printed with a hyaluronic acid bioink, the nanocomposite's increased

strength and improved flow properties allowed for good print fidelity.<sup>[193]</sup> Additionally, rat osteoblast cells remained viable in the printed structure (95%) and showed improved osteogenic differentiation. The increase in cell differentiation was attributed to the steady release of bioactive ions from nanoclay, specifically  $Mg^{2+}$  and  $Si^{4+}$  ions.<sup>[193]</sup>

The ease of incorporating nanoclay into bioinks has also led to an interesting avenue of research for bioprinting: the combination of nanoclay with other bioink reinforcement techniques. Specifically, nanoclay has been used to fabricate a supramolecular, self-healing bioink with hydrogen bonding N-acryloyl glycinamide.<sup>[194]</sup> Nanoclays tuned the viscosity of the bioink, improving printability and reducing swelling. By combining the reversible electrostatic binding of nanoclay with the dual-amide hydrogen bonding of the supramolecular groups, mechanical strength was greatly increased. Finally, *in vivo* studies in rat models revealed that this bioink efficiently promoted new bone formation.<sup>[194]</sup>

Nanoclay have also been combined with GelMA<sup>[103]</sup> and kCA<sup>[192]</sup> to form a nanoengineered bioink. Together, this combination produced a mechanically stable construct via ionic-covalent entanglement (ICE) reinforcement (Fig. 13b).<sup>[195]</sup> This not only improved GelMA's poor printability and mechanical properties, but also demonstrated the combination of the two reinforcement techniques resulted in a synergistic increase in mechanical strength, improving the compressive modulus by over 4-fold. Additionally, a flow model was developed that explored the ability of nanoclay to alter the flow behavior of the bioink. Modeling of the ICE bioink supported a Herschel-Bulkley fluid behavior, demonstrating the low or zero shear stress experienced by the bioink during extrusion. This observation was supported by the high (~90%) cell viability shown in 3D bioprinted structures.<sup>[196]</sup>

Overall, these results illustrate the important contribution that nanoclay can make to the effectiveness of a bioink. Nanoclay incorporation into bioinks can be used to enhance a wide variety of bioink properties, including mechanical strength, printability, drug and protein delivery, osteogenic differentiation, and cell-protective flow properties. These properties, along with their facile incorporation into hydrogels, make nanoclay-based bioinks increasingly popular in 3D printing.

## 8.2. 3D Printing with Hydrogels: Sacrificial Support Bath

Recent studies have shown that nanoclay can be used as a sacrificial support bath for 3D printing.<sup>[197]</sup> The yielding characteristics of nanoclay solution provide a functional support bath material that can maintain a material's extruded shape until solidification occurs post-printing. Furthermore, nanoclay possess thermal stability, transparency (for photo-polymerization), and ionic insensitivity compared to common sacrificial support baths, such as surfactants and poloxamer.<sup>[198]</sup> Nanoclay support baths can assist printing of various materials or composites (e.g. salts).<sup>[198–201]</sup> These support baths stabilize printed constructs by readily flowing when an external force is applied (i.e., higher than the bath's yield stress), such as through a moving extruder.<sup>[199]</sup> Upon motion that surpasses the material's yield stress, the support bath readily flows. This stress induced flow property enables the support bath to fill any crevices in its path and rapidly return to its gel-like behavior. This rapid gelation of the bulk support material retains the shape of any extruded material, successfully

“holding” printed features in place (Fig. 13c).<sup>[199]</sup> This property is specifically beneficial to produce high fidelity prints when gravitational forces and surface tension are lower compared to the yield stress of the support material.<sup>[199]</sup> The entire construct printed within the support bath is able to solidify *in situ* after the application of a suitable crosslinking mechanism. After crosslinking the extruded material in the bath, the construct can subsequently be harvested from the nanoclay bath.

The use of a thixotropic nanoclay support bath is concentration-dependent. Thixotropy is defined as a time-dependent shear thinning property, where application of external force reduces fluid viscosity and allow it to flow. To be used as a printing medium, the colloidal suspension must be able to dispense materials at the needle, but shear upon motion of the extruder. Essentially, too low a concentration does not induce a strong enough thixotropic behavior; however, too high a concentration requires excessive forces to initiate motion of the extruder and produce smooth print surfaces. If a shear gradient is experienced by a material, such as with sacrificial bath extrusion printing, a material’s thixotropic behavior and flow behavior index should be tuned for the linear velocities that the bath experiences during the printing process.<sup>[201]</sup> This rheological analysis confirmed that low concentrations of nanoclay in suspension behave akin to a Newtonian fluid, which is not ideal for a sacrificial bath. However, at concentrations between 1.5 and 3 wt.%, thixotropic behavior was observed with optimal recovery time. Above these concentrations, poor recoverability was observed due to a lack of recovery time and a significant increase in thixotropic index. However, 4 wt.% nanoclay support baths have been used as an optimal concentration for printing gelatin-alginate structures.<sup>[198]</sup>

The feasibility of sacrificial nanoclay support baths has been demonstrated through the ionic crosslinking of alginate, photocrosslinking of SU-8 (an epoxy) and thermal gelation of gelatin.<sup>[199]</sup> When ionically crosslinking alginate,  $\text{CaCl}_2$  is added to the support bath to initiate solidification through divalent cation dissociation. Due to the transparent properties of a nanoclay suspension, fluids, such as SU-8, can be extruded into the support bath then subsequently cured within the bath by exposure to ultraviolet light. Gelatin, a Newtonian fluid when heated above 37 °C, can be extruded within the support bath into complex shapes such as a microvascular network. As the gelatin ink is cooled, the shape of extrusion is maintained and can be harvested from the bath. Utilizing these fabrication conditions, cells such as fibroblasts can be suspended into the hydrogel precursor solution and extruded into complex prints. In addition, the rapid recoverability of the nanoclay suspension allows for printing of these complex structures without any printed supports and in any deposition order (not in precise layer-by-layer fashion). Hollow microvascular channels can also be produced through ‘localized layer-by-layer’ extrusion of both ionic and thermal crosslinking of a alginate and gelatin composite.<sup>[202]</sup> Using a sacrificial nanoclay support bath, complex angles and hollow geometries can be produced, permitting for cellular interactions and perfusion through vascular constructs.

### 8.3. 4D Printing

4D Printing is an emerging technology for fabricating constructs that are dynamic in nature, for example, changing shape or function over time when exposed to an external stimulus

(e.g. temperature, pH, light). The use of “smart” polymers, such as PNIPAM<sup>[203, 204]</sup> or agarose-polyacrylamide<sup>[205]</sup> networks, permit for constructs that change with time (fourth dimension) due to their thermo-reversible properties. However, the innate flow properties of these materials do not permit for fused deposition modeling of high fidelity constructs and are weak in nature. To overcome such limitations, nanoclays are used as an additive to improve the printability of these materials, producing scaffolds with high printability and geometrical accuracy that can change over time.<sup>[204, 205]</sup> For example, the combination of acrylamide into an agarose matrix provides a thermo-responsive smart material.<sup>[205]</sup> However, this precursor solution does not exhibit the thixotropic behavior needed for printing. The incorporation of nanoclay into the precursor system produces thixotropic nanocomposites that can be printed into self-supporting 3D constructs. The addition of nanoclay does not interfere with the basic interactions of the agarose and the chemical bonds of the polyacrylamide. These interactions allow for the nanocomposite precursor to be extruded into complex shapes while enabling a fourth dimensional change to the matrix through a rapid thermal-reversible sol-gel transition provided by the agarose network. At high temperatures, the agarose is disrupted into flexible chains while the polyacrylamide maintains its chemical network. This enables these gels to be heated and manipulated into various shapes that can be hardened and maintained at ambient temperatures. This process can be repeated while still maintaining a high cell viability of around 90%.

PNIPAM is a common “smart” material, responding to both light (near-infrared light) and temperature (LCST  $\sim 32^{\circ}\text{C}$ ), yet lacks the flow properties to produce 3D constructs. As a result, 4D printed constructs are limited; however, the combination of nanoclay in the NIPAM precursor serves as an effective rheological additive to improve the printability of this thermo-responsive hydrogel while maintaining the responsive functionality of the NIPAM. Nanoclay serves as a physical crosslinker within the system, enhancing the interactions between polymer chains and the fidelity of printed constructs without any solidification during the printing process. Other nanoparticles, such as graphene oxide, gold nanorods, or carbon nanotubes, can also be incorporated in to the composite to raise the temperature sensitivity of the overall scaffold due to their excellent photothermal conversion and thermal conductivity. The addition of these nanoparticles allows specific absorption and conversion of near-infrared light into thermal energy, initiating a response within the printed construct.<sup>[206]</sup>

In addition to the swelling and deswelling of PNIPAM-nanoclay networks through diverse stimuli, thermo-responses generated from the 3D construct can also be controlled through extrusion directions. Specifically, the ink combination of NIPAM, nanoclay, glucose oxidase, glucose, and nanofibrillated cellulose can be extruded in various directions, causing shear-induced, anisotropic orientation of the cellulose fibrils.<sup>[204]</sup> One study showed that printing of the bioink into specific anisotropic patterns can induce specific response to external stimuli, therefore mimicking the functional folding of flower architectures (Fig. 13d).<sup>[204]</sup> This anisotropic alignment of the cellulose caused varied swelling strains and elastic moduli in the longitudinal and transverse directions, but was dependent on the printing speed and needle gauge. By altering the flow parameters to induce various shears, the scaffolds water uptake varied by the extent of orientation, inducing a change in shape.

Overall, this 4D printing system relies on the material and geometry produced by extrusion that can be controlled in space and time through the incorporation of nanoclay.

## 9. Conclusion

Nanoclay usage has continued to expand since their initial discovery over 4000 years ago. Nanoclays are an emerging class of biomaterials with unique layered shape, nanosize, and well-defined structure. These atomically thin nanoclays have heterogeneous charge distribution and patchy interactions that enable the physical interactions of nanoclay with a range of biomolecules, polymers, and biological components. Nanoclays show high cytocompatibility and biocompatibility compared to other classes of nanomaterials. In addition, nanoclays possess inherent bioactive properties and have been used for a range of tissue engineering applications including bone, cartilage, osteochondral, tissue sealants, wound healing, hemostats, and organoid formation. Due to high surface area and charged characteristics, nanoclays interact with range of small and large biomolecules and have been used for sustained and prolonged delivery of therapeutics. Nanoclays form an empty gel phase that can be combined with various natural and synthetic polymers to obtain shear-thinning biomaterials. These shear-thinning characteristics have been used for range of additive manufacturing approaches including 3D/4D printing. Overall, it is expected that this class of biomaterials can serve as an important technology platform for multiple biomedical applications.

## 10. Future Perspective

2D nanoclays are an emerging class of biomaterials due to their unique ability to interact with a range of polymers, and macromolecules. Nanoclays have shown high cytocompatibility and biocompatibility. A range of biomedical applications for nanoclay have been investigated, including orthopedic tissue engineering, wound healing, and hemostats, amongst others. Future studies will focus on translating these approaches towards clinical applications. For example, nanoclays were shown to have osteoinductive properties and can be used to reduce the amount of growth factors required for bone regeneration. The osteoinductive characteristics of nanoclay-based technology can be extended to load-bearing applications by combining with interbody fusion cages or biodegradable implants made from poly(propylene fumarate) (PPF) or poly(L-lactic acid) (PLA) or polycaprolactone (PCL)<sup>[24, 207]</sup> or poly(butylene terephthalate) (PBT)<sup>[208]</sup>.

The interaction of nanoclay with cells is not fully understood, and only few recent studies have attempted to shed light on these interactions. In future it is expected that omics-based approaches such as transcriptomics, proteomics, and metabolomics will be used to determine the interactions between nanoclay and cells. These approaches will provide an unbiased “global” view of the cellular activities affected by nanoclay treatment. As nanoclays are composed of mineral ions, it is also important to determine the effect of ionic dissolution products on cells, as well as the therapeutic potential of these released ions. The effects of ionic dissolution products on osteogenesis, chondrogenesis, and angiogenesis should also be investigated in detail.

Another exciting application of nanoclay is in organoids and immune engineering. The use of nanoclay-based materials for organoid culture will be interesting to investigate. Nanoclays have the ability to interact with immune cells, but it is not clear why and how nanoclays have immunomodulatory properties. It would be valuable to investigate this phenomenon further for potential applications in immunoengineering.

Our ability to understand the interactions between nanoclays, polymers, and biological moieties is continuously expanding with improved imaging, modeling, and sensing techniques. Potential applications of nanoclay-based materials in cells sheet engineering for long-term culturing of stem cells and induced pluripotent stem cells (iPSCs) will be interesting to evaluate. Moreover, as nanoclays have the ability to induce differentiation of multipotent cells, it is also important to investigate the effect of nanoclay on pluripotent cells.

To induce robust differentiation, growth factors, transcription factors or cytokines can be released from nanoclay based biomaterials. As the interactions between macromolecules and nanoclay become more well-defined, therapeutic delivery strategies will become more robust and effective. This will have widespread applications for nanoclay in regenerative medicine. As nanoclays interact with biomolecules through electrostatic interactions, it is important to determine if they prefer to sequester specific type of proteins. The composition of proteins that coat the nanoclay surface over time, in consideration of the Vroman effect, needs to be elucidated. Other promising research directions will involve the use of nanoclay for targeted delivery of therapeutics.

Computational modelling will likely be used to better predict physical properties and interactions of nanoclay and polymer. Previous studies have used Monte Carlo modelling to predict the interactions between nanoclay, and can potentially estimate nanoclay/polymer interactions. By understanding these interactions, custom inks for 3D printing can be designed. Predicting the flow behavior of nanoclay-based inks can help to design inks that can shield encapsulated cells from mechanical deformation. This approach can improve cell viability and promote regenerative medicine approaches.

As current nanoclays have predefined structure and chemistry, there significant room to develop nanoclays with custom chemical formulations or size. For example, changes in the shape, size, and ionic composition of nanoclays could lead to new avenues for directing cell behavior or differentiation. Moreover, the changes to particle size could affect cellular uptake and changes to the ionic composition could affect the surface charge which dictates protein adsorption. In addition, these physical and chemical changes in nanoclay could affect interactions with polymers, potentially improving current bioink development. Nanoclays present an ideal platform for introducing small modifications to produce unique and specific nanoclays for desired biomedical applications.

### **Acknowledgment:**

The author apologizes to all colleagues whose work could not be cited because of space constraints. The manuscript was written through contributions of all authors. All authors have given approval to the final version of the manuscript. We are grateful to John Grime for editorial suggestions on the manuscript and David Chimene for technical input on additive manufacturing section. Research reported in this publication was supported by the



National Institute of Biomedical Imaging and Bioengineering (NIBIB) of the National Institutes of Health (NIH) Director's New Innovator Award (DP2 EB026265) and the National Science Foundation (NSF) Award (CBET 1705852). The content is solely the responsibility of the authors and does not necessarily represent the official views of the funding agency.

Dr. Akhilesh K. Gaharwar is an assistant professor in the Department of Biomedical Engineering at Texas A&M University. The goal of his lab is to understand the cell-nanomaterials interactions and to develop nanoengineered strategies for modulating stem cell behavior for repair and regeneration of damaged tissue. His research is funded by the National Institute of Health (NIH), the National Science Foundation (NSF) and corporate sponsors. He co-authored more than 100 journal articles in high impact journals including *Advanced Materials*, *PNAS*, *ACS Nano*, and *Biomaterials*. He also edited two books on nanomaterials and microscale technologies. He serves on the editorial board of leading biomaterial and regenerative medicine journals. He has received several distinctions, including the NIH Director's New Innovator Award (DP2), Dean of Excellence Award by CoE, CMBE-BMES Rising Star Award, CMBE Young Innovator Award, Outstanding Faculty Mentor Award, and Dimitris Chorafas Foundation Award.

## References

- [1]. Bergaya F, Theng BKG, Lagaly G, Handbook of clay science, Vol. 1, Elsevier, 2006; Guggenheim s., Martin RT, Clay Minerals 2018, 30, 257.
- [2]. Dawson JI, Oreffo RO, *Adv Mater* 2013, 25, 4069. [PubMed: 23722321]
- [3]. Murray HH, *Applied Clay Science* 2000, 17, 207.
- [4]. B. Additives, 2019.
- [5]. Neumann BS, 1971; Neumann BS, 1972; Wright AC, Rupert JP, Google Patents, 1977.
- [6]. Davila JL, d'Avila MA, *Carbohydr Polym* 2017, 157, 1; Mourchid A, Delville A, Lambard J, LeColier E, Levitz P, *Langmuir* 1995, 11, 1942; Nelson A, Cosgrove T, *Langmuir* 2004, 20, 2298. [PubMed: 27987800]
- [7]. Mongondry P, Tassin JF, Nicolai T, *J Colloid Interface Sci* 2005, 283, 397. [PubMed: 15721911]
- [8]. Ruzicka B, Zaccarelli E, *Soft Matter* 2011, 7, 1268.
- [9]. Thompson DW, Butterworth JT, *Journal of Colloid and Interface Science* 1992, 151, 236.
- [10]. Rosta L, von Gunten HR, *Journal of Colloid and Interface Science* 1990, 134, 397.
- [11]. Mourchid A, Delville A, Levitz P, *Faraday Discussions* 1995, 101, 275.
- [12]. Mourchid A, Delville A, Lambard J, Lecolier E, Levitz P, *Langmuir* 1995, 11, 1942.
- [13]. Carrow JK, Cross LM, Reese RW, Jaiswal MK, Gregory CA, Kaunas R, Singh I, Gaharwar AK, *Proc Natl Acad Sci U S A* 2018, 115, E3905. [PubMed: 29643075]
- [14]. Rosta L, Vongunten HR, *Journal of Colloid and Interface Science* 1990, 134, 397.
- [15]. Dijkstra M, Hansen JP, Madden PA, *Phys Rev Lett* 1995, 75, 2236. [PubMed: 10059248]
- [16]. Sheikhi A, Afewerki S, Oklu R, Gaharwar AK, Khademhosseini A, *Biomater Sci* 2018, 6, 2073. [PubMed: 29944151]
- [17]. Herrera NN, Letoffe J-M, Putaux J-L, David L, Bourgeat-Lami E, *Langmuir* 2004, 20, 1564.
- [18]. Lan T, Kaviratna PD, Pinnavaia TJ, *Chemistry of Materials* 1995, 7, 2144.
- [19]. De Paiva LB, Morales AR, Díaz FRV, *Applied clay science* 2008, 42, 8.
- [20]. Fu Y-T, Heinz H, *Chemistry of Materials* 2010, 22, 1595; Choi JH, Park YW, Park TH, Song EH, Lee HJ, Kim H, Shin SJ, Fai VL, Ju BK, *Langmuir* 2012, 28, 6826.
- [21]. Park J, Jana SC, *Macromolecules* 2003, 36, 8391.
- [22]. Savenko V, Bulavin L, Rawiso M, Loginov M, Vorobiev E, Lebovka NI, *Phys Rev E Stat Nonlin Soft Matter Phys* 2013, 88, 052301.
- [23]. Kim YJ, Liu YD, Choi HJ, Park SJ, *J Colloid Interface Sci* 2013, 394, 108; Sun Q, Deng Y, Wang ZL, *Macromolecular Materials and Engineering* 2004, 289, 288. [PubMed: 23332941]
- [24]. Gaharwar AK, Mukundan S, Karaca E, Dolatshahi-Pirouz A, Patel A, Rangarajan K, Mihaila SM, Iviglia G, Zhang H, Khademhosseini A, *Tissue Engineering Part A* 2014, 20, 2088. [PubMed: 24842693]
- [25]. Ruzicka B, Zaccarelli E, Zulian L, Angelini R, Sztucki M, Moussaid A, Narayanan T, Sciortino F, *Nat Mater* 2011, 10, 56. [PubMed: 21151164]

- [26]. Ruzicka B, Zaccarelli E, Zulian L, Angelini R, Sztucki M, Moussaïd A, Narayanan T, Sciortino F, Nature materials 2011, 10, 56. [PubMed: 21151164]
- [27]. Nicolai T, Cocard S, Langmuir 2000, 16, 8189.
- [28]. Avery RG, Ramsay JDF, Journal of Colloid and Interface Science 1986, 109, 448.
- [29]. Takeda M, Matsunaga T, Nishida T, Endo H, Takahashi T, Shibayama M, Macromolecules 2010, 43, 7793; Mori Y, Togashi K, Nakamura K, Advanced Powder Technology 2001, 12, 45.
- [30]. Levitz P, Lecolier E, Mourchid A, Delville A, Lyonnard S, Europhysics Letters (EPL) 2000, 49, 672.
- [31]. Levitz P, Lecolier E, Mourchid A, Delville A, Lyonnard S, Europhysics Letters 2000, 49, 672.
- [32]. Sheikhi A, Afewerki S, Oklu R, Gaharwar AK, Khademhosseini A, Biomater. Sci. 2018, 6, 2073. [PubMed: 29944151]
- [33]. Ruzicka B, Zulian L, Ruocco G, Philosophical Magazine 2007, 87, 449.
- [34]. Jatav S, Joshi YM, Applied Clay Science 2014, 97–98, 72.
- [35]. Thuresson A, Segad M, Plivelic TS, Skepö M, The Journal of Physical Chemistry C 2017, 121, 7387.
- [36]. Dijkstra M, Hansen J, Madden P, Physical review letters 1995, 75, 2236. [PubMed: 10059248]
- [37]. Dijkstra M, Hansen J-P, Madden PA, Physical Review E 1997, 55, 3044.
- [38]. Shahin A, Joshi YM, Langmuir 2012, 28, 15674. [PubMed: 23057660]
- [39]. Shi P, Kim YH, Mousa M, Sanchez RR, Oreffo ROC, Dawson JI, Adv Healthc Mater 2018, 7, e1800331.
- [40]. Jatav S, Joshi YM, Applied Clay Science 2014, 97–98, 72.
- [41]. Jabbari-Farouji S, Tanaka H, Wegdam GH, Bonn D, Phys Rev E Stat Nonlin Soft Matter Phys 2008, 78, 061405.
- [42]. Zreiqat H, Howlett CR, Zannettino A, Evans P, Schulze-Tanzil G, Knabe C, Shakibaei M, J Biomed Mater Res 2002, 62, 175. [PubMed: 12209937]
- [43]. Carlier MF, Valentin-Ranc C, Combeau C, Fievez S, Pantoloni D, Adv Exp Med Biol 1994, 358, 71; Valentinranc C, Carlier MF, J Biol Chem 1991, 266, 7668. [PubMed: 7801813]
- [44]. Clement-Lacroix P, Ai M, Morvan F, Roman-Roman S, Vayssiere B, Belleville C, Estrera K, Warman ML, Baron R, Rawadi G, Proc Natl Acad Sci U S A 2005, 102, 17406. [PubMed: 16293698]
- [45]. Zhang F, Phiel CJ, Spece L, Gurvich N, Klein PS, J Biol Chem 2003, 278, 33067. [PubMed: 12796505]
- [46]. Clevers H, Cell 2006, 127, 469. [PubMed: 17081971]
- [47]. Baghaban Eslaminejad M, Karimi N, Shahhoseini M, Cell J 2011, 13, 117. [PubMed: 23508136]
- [48]. Hoppe A, Guldal NS, Boccaccini AR, Biomaterials 2011, 32, 2757; Zhai W, Lu H, Chen L, Lin X, Huang Y, Dai K, Naoki K, Chen G, Chang J, Acta Biomater 2012, 8, 341. [PubMed: 21292319]
- [49]. Reffitt DM, Ogston N, Jugdaohsingh R, Cheung HF, Evans BA, Thompson RP, Powell JJ, Hampson GN, Bone 2003, 32, 127. [PubMed: 12633784]
- [50]. Nel AE, Madler L, Velegol D, Xia T, Hoek EM, Somasundaran P, Klaessig F, Castranova V, Thompson M, Nat Mater 2009, 8, 543. [PubMed: 19525947]
- [51]. Cedervall T, Lynch I, Lindman S, Berggard T, Thulin E, Nilsson H, Dawson KA, Linse S, Proc Natl Acad Sci U S A 2007, 104, 2050. [PubMed: 17267609]
- [52]. Cross LM, Carrow JK, Ding X, Singh KA, Gaharwar AK, ACS Appl Mater Interfaces 2019.
- [53]. Nguyen VH, Lee BJ, Int J Nanomedicine 2017, 12, 3137. [PubMed: 28458536]
- [54]. Gaharwar AK, Mihaila SM, Swami A, Patel A, Sant S, Reis RL, Marques AP, Gomes ME, Khademhosseini A, Adv Mater 2013, 25, 3329. [PubMed: 23670944]
- [55]. Mihaila SM, Gaharwar AK, Reis RL, Khademhosseini A, Marques AP, Gomes ME, Biomaterials 2014, 35, 9087. [PubMed: 25123923]
- [56]. Doyon JB, Zeitler B, Cheng J, Cheng AT, Cherone JM, Santiago Y, Lee AH, Vo TD, Doyon Y, Miller JC, Paschon DE, Zhang L, Rebar EJ, Gregory PD, Urnov FD, Drubin DG, Nat Cell Biol 2011, 13, 331. [PubMed: 21297641]

- [57]. Rawlings JS, Rosler KM, Harrison DA, J Cell Sci 2004, 117, 1281; Cantley LC, Science 2002, 296, 1655. [PubMed: 15020666]
- [58]. Liu Y, Meng H, Konst S, Sarmiento R, Rajachar R, Lee BP, ACS Appl Mater Interfaces 2014, 6, 16982. [PubMed: 25222290]
- [59]. Liu Y, Meng H, Qian Z, Fan N, Choi W, Zhao F, Lee B, Angewandte Chemie International Edition 2017, 56, 4224. [PubMed: 28296024]
- [60]. Boyer C, Figueiredo L, Pace R, Lesoeur J, Rouillon T, Le Visage C, Tassin J-F, Weiss P, Guicheux J, Rethore G, Acta biomaterialia 2018, 65, 112; Shikinaka K, Aizawa K, Murakami Y, Osada Y, Tokita M, Watanabe J, Shigehara K, J Colloid Interface Sci 2012, 369, 470. [PubMed: 29128532]
- [61]. Schmidt G, Nakatani AI, Han CC, Rheologica Acta 2002, 41, 45.
- [62]. Schmidt G, Nakatani AI, Butler PD, Han CC, Macromolecules 2002, 35, 4725.
- [63]. Cedervall T, Lynch I, Lindman S, Berggard T, Thulin E, Nilsson H, Dawson KA, Linse S, P Natl Acad Sci USA 2007, 104, 2050; Nel AE, Madler L, Velegol D, Xia T, Hoek EMV, Somasundaran P, Klaessig F, Castranova V, Thompson M, Nature Materials 2009, 8, 543; Schexnailder P, Schmidt G, Colloid and Polymer Science 2009, 287, 1.
- [64]. Gaharwar AK, Schexnailder PJ, Dundigalla A, White JD, Matos-Perez CR, Cloud JL, Seifert S, Wilker JJ, Schmidt G, Macromol Rapid Commun 2011, 32, 50. [PubMed: 21432969]
- [65]. Gaharwar AK, Peppas NA, Khademhosseini A, Biotechnol Bioeng 2014, 111, 441; Dawson JJ, Oreffo ROC, Adv. Mater. 2013, 25, 4069. [PubMed: 24264728]
- [66]. Wang Q, Mynar JL, Yoshida M, Lee E, Lee M, Okuro K, Kinbara K, Aida T, Nature 2010, 463, 339. [PubMed: 20090750]
- [67]. Gaharwar AK, Peppas NA, Khademhosseini A, Biotechnology and bioengineering 2014, 111, 441. [PubMed: 24264728]
- [68]. Guvendiren M, Lu HD, Burdick JA, Soft Matter 2012, 8, 260; Yu L, Ding J, Chem Soc Rev 2008, 37, 1473; Li Y, Rodrigues J, Tomas H, Chem Soc Rev 2012, 41, 2193.
- [69]. Pilavtepe M, Recktenwald SM, Schuhmann R, Emmerich K, Willenbacher N, Journal of Rheology 2018, 62, 593.
- [70]. Dávila JL, d'Ávila MA, Carbohydrate Polymers 2017, 157, 1. [PubMed: 27987800]
- [71]. Wang Q, Mynar JL, Yoshida M, Lee E, Lee M, Okuro K, Kinbara K, Aida T, Nature 2010, 463, 339. [PubMed: 20090750]
- [72]. Schmidt G, Nakatani AI, Butler PD, Han CC, Macromolecules 2002, 35, 4725.
- [73]. Nelson A, Cosgrove T, Langmuir 2004, 20, 2298. [PubMed: 15835687]
- [74]. Nelson A, Cosgrove T, Langmuir 2004, 20, 10382. [PubMed: 15544363]
- [75]. Nelson A, Cosgrove T, Langmuir 2005, 21, 9176; Wu C-J, Gaharwar AK, Chan BK, Schmidt G, Macromolecules 2011, 44, 8215; Boucenna I, Royon L, Colinar P, Guedeau-Boudeville MA, Mourchid A, Langmuir 2010, 26, 14430. [PubMed: 16171348]
- [76]. Haraguchi K, Xu Y, Colloid and Polymer Science 2012, 290, 1627; Haraguchi K, Xu Y, Li G, Macromol Rapid Commun 2010, 31, 718; Haraguchi K, Li HJ, Icafp, Ultra-high hydrophobicity on the surface of nanocomposite hydrogels with a poly(n-isopropylacrylamide)/clay network, 2009.
- [77]. Pawar N, Bohidar HB, J Chem Phys 2009, 131, 045103.
- [78]. Thakur A, Jaiswal MK, Peak CW, Carrow JK, Gentry J, Dolatshahi-Pirouz A, Gaharwar AK, Nanoscale 2016, 8, 12362. [PubMed: 27270567]
- [79]. Nelson A, Cosgrove T, Langmuir 2004, 20, 10382. [PubMed: 15544363]
- [80]. Nelson A, Cosgrove T, Langmuir 2005, 21, 9176. [PubMed: 16171348]
- [81]. Haraguchi K, Li H-J, Matsuda K, Takehisa T, Elliott E, Macromolecules 2005, 38, 3482; Fukasawa M, Sakai T, Chung U.-i., Haraguchi K, Macromolecules 2010, 43, 4370; Haraguchi K, Xu YJ, Colloid and Polymer Science 2012, 290, 1627.
- [82]. Ebato M, Takehisa T, Haraguchi K, Adv Mater 2006, 18, 2250.
- [83]. Haraguchi K, Xu YJ, Li G, Macromolecular Rapid Communications 2010, 31, 718. [PubMed: 21590961]

- [84]. Lorthioir C, Khalil M, Wintgens V, Amiel C, Langmuir 2012, 28, 7859. [PubMed: 22512344]
- [85]. Lorthioir C, Khalil M, Wintgens V, Amiel C, Langmuir 2012, 28, 7859. [PubMed: 22512344]
- [86]. Peak CW, Stein J, Gold KA, Gaharwar AK, Langmuir 2018, 34, 917. [PubMed: 28981287]
- [87]. Nelson A, Cosgrove T, Langmuir 2004, 20, 10382. [PubMed: 15544363]
- [88]. Varade D, Haraguchi K, Langmuir 2013, 29, 1977; Haraguchi K, Li HJ, Matsuda K, Takehisa T, Elliott E, Macromolecules 2005, 38, 3482; Fukasawa M, Sakai T, Chung UI, Haraguchi K, Macromolecules 2010, 43, 4370. [PubMed: 23343394]
- [89]. Pawar N, Bohidar HB, The Journal of Chemical Physics 2009, 131, 045103.
- [90]. Gaharwar AK, Kishore V, Rivera C, Bullock W, Wu CJ, Akkus O, Schmidt G, Macromol Biosci 2012, 12, 779. [PubMed: 22517665]
- [91]. Mohanty B, Gupta A, Bohidar HB, Bandyopadhyay S, Journal of Polymer Science Part B: Polymer Physics 2007, 45, 1511.
- [92]. Sheikhi A, Afewerki S, Oklu R, Gaharwar AK, Khademhosseini A, Biomaterials Science 2018, 6, 2073. [PubMed: 29944151]
- [93]. Langer R, Vacanti JP, Science 1993, 260, 920. [PubMed: 8493529]
- [94]. Zreiqat H, Howlett CR, Zannettino A, Evans P, Schulze-Tanzil G, Knabe C, Shakibaei M, J Biomed Mater Res 2002, 62, 175. [PubMed: 12209937]
- [95]. Shi P, Kim Y-H, Mousa M, Sanchez RR, Oreffo ROC, Dawson JI, Advanced Healthcare Materials 2018, 1800331, 1.
- [96]. Wang C, Wang S, Li K, Ju Y, Li J, Zhang Y, Li J, Liu X, Shi X, Zhao Q, PLOS ONE 2014, 9, e99585.
- [97]. Amini AR, Laurencin CT, Nukavarapu SP, Crit Rev Biomed Eng 2012, 40, 363. [PubMed: 23339648]
- [98]. Gaharwar AK, Schexnaider PJ, Kline BP, Schmidt G, Acta Biomaterialia 2011, 7, 568. [PubMed: 20854941]
- [99]. Keratitayanan P, Tatullo M, Khariton M, Joshi P, Perniconi B, Gaharwar AK, ACS Biomaterials Science & Engineering 2017, 3, 590; Keratitayanan P, Gaharwar AK, Acta Biomater 2015, 26, 34.
- [100]. Wang S, Castro R, An X, Song C, Luo Y, Shen M, Tomás H, Zhu M, Shi X, Journal of Materials Chemistry 2012, 22, 23357.
- [101]. Wang S, Castro R, An X, Song C, Luo Y, Shen M, Tomas H, Zhu M, Shi X, Journal of Materials Chemistry 2012, 22, 23357.
- [102]. Xavier JR, Thakur T, Desai P, Jaiswal MK, Sears N, Cosgriff-Hernandez E, Kaunas R, Gaharwar AK, ACS Nano 2015, 9, 3109. [PubMed: 25674809]
- [103]. Xavier JR, Thakur T, Desai P, Jaiswal MK, Sears N, Cosgriff-Hernandez E, Kaunas R, Gaharwar AK, ACS Nano 2015, 9, 3109. [PubMed: 25674809]
- [104]. Paul A, Manoharan V, Krafft D, Assmann A, Uquillas JA, Shin SR, Hasan A, Hussain MA, Memic A, Gaharwar AK, Khademhosseini A, J Mater Chem B 2016, 4, 3544. [PubMed: 27525102]
- [105]. Paul A, Manoharan V, Krafft D, Assmann A, Uquillas JA, Shin SR, Hasan A, Hussain MA, Memic A, Gaharwar AK, Khademhosseini A, Journal of Materials Chemistry B 2016, 4, 3544. [PubMed: 27525102]
- [106]. Basu S, Pacelli S, Feng Y, Lu Q, Wang J, Paul A, ACS nano 2018.
- [107]. Tao L, Zhonglong L, Ming X, Zezheng Y, Zhiyuan L, Xiaojun Z, Jinwu W, RSC Advances 2017, 7, 54100.
- [108]. Tao L, Zhonglong L, Ming X, Zezheng Y, Zhiyuan L, Xiaojun Z, Jinwu W, Rsc Adv 2017, 7, 54100.
- [109]. Ahlfeld T, Cidonio G, Kilian D, Duin S, Akkineni AR, Dawson JI, Yang S, Lode A, Oreffo ROC, Gelinsky M, Biofabrication 2017, 9, 034103.
- [110]. Iwamoto M, Ohta Y, Larmour C, Enomoto-Iwamoto M, Birth Defects Res C Embryo Today 2013, 99, 192; Makris EA, Gomoll AH, Malizos KN, Hu JC, Athanasiou KA, Nat Rev Rheumatol 2015, 11, 21. [PubMed: 24078496]

- [111]. Mackay AM, Beck SC, Murphy JM, Barry FP, Chichester CO, Pittenger MF, Tissue Eng 1998, 4, 415; Benya PD, Padilla SR, Nimni ME, Cell 1978, 15, 1313; Gao L, McBeath R, Chen CS, Stem Cells 2010, 28, 564; Vega SL, Kwon MY, Burdick JA, Eur Cell Mater 2017, 33, 59. [PubMed: 9916173]
- [112]. Eslahi N, Abdorahim M, Simchi A, Biomacromolecules 2016, 17, 3441. [PubMed: 27775329]
- [113]. Vega SL, Kwon MY, Burdick JA, Eur Cells Mater 2017, 33, 59.
- [114]. Thakur A, Jaiswal MK, Peak CW, Carrow JK, Gentry J, Dolatshahi-Pirouz A, Gaharwar AK, Nanoscale 2016, 8, 12362. [PubMed: 27270567]
- [115]. Wilson SA, Cross LM, Peak CW, Gaharwar AK, ACS Appl Mater Interfaces 2017, 9, 43449. [PubMed: 29214803]
- [116]. Boyer C, Figueiredo L, Pace R, Lesoeur J, Rouillon T, Visage CL, Tassin JF, Weiss P, Guicheux J, Rethore G, Acta Biomater 2018, 65, 112. [PubMed: 29128532]
- [117]. Boyer C, Figueiredo L, Pace R, Lesoeur J, Rouillon T, Le Visage C, Tassin JF, Weiss P, Guicheux J, Rethore G, Acta Biomater 2018, 65, 112. [PubMed: 29128532]
- [118]. Bryant SJ, Anseth KS, J Biomed Mater Res A 2003, 64, 70. [PubMed: 12483698]
- [119]. Nojoomi A, Tamjid E, Simchi A, Bonakdar S, Stroeve P, Int J Polym Mater Po 2016, 66, 105.
- [120]. Wu CJ, Gaharwar AK, Chan BK, Schmidt G, Macromolecules 2011, 44, 8215.
- [121]. Eslahi N, Simchi A, Mehrjoo M, Shokrgozar MA, Bonakdar S, RSC Advances 2016, 6, 62944.
- [122]. Cross LM, Thakur A, Jalili NA, Detamore M, Gaharwar AK, Acta Biomater 2016, 42, 2. [PubMed: 27326917]
- [123]. Cross LM, Shah K, Palani S, Peak CW, Gaharwar AK, Nanomedicine : nanotechnology, biology, and medicine 2018, 14, 2465.
- [124]. Hesel U, Dahmen C, Kessler H, Biomaterials 2003, 24, 4385; Ito Y, Biomaterials 1999, 20, 2333. [PubMed: 12922151]
- [125]. Schexnailder PJ, Gaharwar AK, Bartlett RL 2nd, Seal BL, Schmidt G, Macromol Biosci 2010, 10, 1416; Gaharwar AK, Schexnailder PJ, Jin Q, Wu CJ, Schmidt G, ACS Appl Mater Interfaces 2010, 2, 3119. [PubMed: 20602416]
- [126]. S. P. J, G. A. K, B. I. R. L, S. B. L, Gudrun S, Macromolecular Bioscience 2010, 10, 1416. [PubMed: 20602416]
- [127]. Chang C-W, van Spreeuwel A, Zhang C, Varghese S, Soft Matter 2010, 6, 5157.
- [128]. Gaharwar AK, Rivera CP, Wu CJ, Schmidt G, Acta Biomater 2011, 7, 4139. [PubMed: 21839864]
- [129]. Gaharwar AK, Rivera CP, Wu C-J, Schmidt G, Acta Biomater 2011, 7, 4139. [PubMed: 21839864]
- [130]. Haraguchi K, Masatoshi S, Kotobuki N, Murata K, J Biomater Sci Polym Ed 2011, 22, 2389. [PubMed: 21118632]
- [131]. Haraguchi K, Journal of Stem Cells & Regenerative Medicine 2012, 8, 2. [PubMed: 24693187]
- [132]. Haraguchi K, Takehisa T, Ebato M, Biomacromolecules 2006, 7, 3267. [PubMed: 17096560]
- [133]. Haraguchi K, Takehisa T, Ebato M, Biomacromolecules 2006, 7, 3267. [PubMed: 17096560]
- [134]. Liu Y, Meng H, Konst S, Sarmiento R, Rajachar R, Lee BP, ACS Applied Materials & Interfaces 2014, 6, 16982. [PubMed: 25222290]
- [135]. Bucalo B, Eaglstein WH, Falanga V, Wound Repair Regen 1993, 1, 181. [PubMed: 17163887]
- [136]. Beldon P, Surgery (Oxford) 2010, 28, 409.
- [137]. Ghadiri M, Chrzanowski W, Rohanizadeh R, Journal of Materials Science: Materials in Medicine 2014, 25, 2513. [PubMed: 25027303]
- [138]. Li T, Liu ZL, Xiao M, Yang ZZ, Peng MZ, Li CD, Zhou XJ, Wang JW, Stem Cell Res Ther 2018, 9, 100. [PubMed: 29642953]
- [139]. Ghadiri M, Chrzanowski W, Lee W, Rohanizadeh R, RSC Advances 2014, 4, 35332.
- [140]. Kiaee G, Mostafalu P, Samandari M, Sonkusale S, Adv Healthc Mater 2018, 7, e1800396.
- [141]. Kiaee G, Mostafalu P, Samandari M, Sonkusale S, Advanced Healthcare Materials 2018, 7, 1800396.
- [142]. Guvendiren M, Lu H, Burdick J, Soft matter 2012, 8, 260.

- [143]. Koehler J, Brandl FP, Goepferich AM, European Polymer Journal 2018, 100, 1.
- [144]. Golafshan N, Rezahasani R, Esfahani MT, Kharaziha M, Khorasani S, Carbohydrate polymers 2017, 176, 392. [PubMed: 28927623]
- [145]. Huang K-T, Fang Y-L, Hsieh P-S, Li C-C, Dai N-T, Huang C-J, Journal of Materials Chemistry B 2016, 4, 4206.
- [146]. Gaharwar AK, Avery RK, Assmann A, Paul A, McKinley GH, Khademhosseini A, Olsen BD, ACS Nano 2014, 8, 9833; Avery RK, Albadawi H, Akbari M, Zhang YS, Duggan MJ, Sahani DV, Olsen BD, Khademhosseini A, Oklu R, Sci Transl Med 2016, 8, 365ra156. [PubMed: 25221894]
- [147]. Gaharwar AK, Avery RK, Assmann A, Paul A, McKinley GH, Khademhosseini A, Olsen BD, ACS Nano 2014, 8, 9833. [PubMed: 25221894]
- [148]. Avery RK, Albadawi H, Akbari M, Zhang YS, Duggan MJ, Sahani DV, Olsen BD, Khademhosseini A, Oklu R, Science Translational Medicine 2016, 8, 365ra156.
- [149]. Lokhande G, Carrow JK, Thakur T, Xavier JR, Parani M, Bayless KJ, Gaharwar AK, Acta Biomater 2018, 70, 35. [PubMed: 29425720]
- [150]. Lokhande G, Carrow JK, Thakur T, Xavier JR, Parani M, Bayless KJ, Gaharwar AK, Acta Biomaterialia 2018, 70, 35. [PubMed: 29425720]
- [151]. Davie EW, Fujikawa K, Kisiel W, Biochemistry 1991, 30, 10363; Naito K, Fujikawa K, J Biol Chem 1991, 266, 7353. [PubMed: 1931959]
- [152]. Rybakowski JK, Human Psychopharmacology: Clinical and Experimental 1999, 14, 345.
- [153]. Tam M, Gomez S, Gonzalez-Gross M, Marcos A, Eur J Clin Nutr 2003, 57, 1193. [PubMed: 14506478]
- [154]. Li B, Cao H, Zhao Y, Cheng M, Qin H, Cheng T, Hu Y, Zhang X, Liu X, Sci Rep 2017, 7, 42707. [PubMed: 28198427]
- [155]. Koo H, Ryu SH, Ahn HJ, Jung WK, Park YK, Kwon NH, Kim SH, Kim JM, Yoo BW, Choi SI, Davis WC, Park YH, Clin Vaccine Immunol 2006, 13, 1255; Yoo BW, Choi SI, Kim SH, Yang SJ, Koo HC, Seo SH, Park BK, Yoo HS, Park YH, Journal of veterinary science 2001, 2, 15. [PubMed: 16943344]
- [156]. Jurkic LM, Cepanec I, Pavelic SK, Pavelic K, Nutr Metab (Lond) 2013, 10, 2. [PubMed: 23298332]
- [157]. Li T, Liu ZL, Xiao M, Yang ZZ, Peng MZ, Di Li C, Zhou XJ, Wang JW, Stem cell research & therapy 2018, 9, 100. [PubMed: 29642953]
- [158]. Purwada A, Jaiswal MK, Ahn H, Nojima T, Kitamura D, Gaharwar AK, Cerchiotti L, Singh A, Biomaterials 2015, 63, 24. [PubMed: 26072995]
- [159]. Purwada A, Singh A, Nat Protoc 2017, 12, 168. [PubMed: 28005068]
- [160]. Purwada A, Singh A, nature protocols 2017, 12, 168. [PubMed: 28005068]
- [161]. Wang G, Maciel D, Wu Y, Rodrigues J, Shi X, Yuan Y, Liu C, Tomas H, Li Y, ACS Appl Mater Interfaces 2014, 6, 16687; Wang S, Wu Y, Guo R, Huang Y, Wen S, Shen M, Wang J, Shi X, Langmuir 2013, 29, 5030; Goncalves M, Figueira P, Maciel D, Rodrigues J, Qu X, Liu C, Tomas H, Li Y, Acta Biomater 2014, 10, 300. [PubMed: 25167168]
- [162]. Wu Y, Guo R, Wen S, Shen M, Zhu M, Wang J, Shi X, Journal of Materials Chemistry B 2014, 2, 7410.
- [163]. Aguzzi C, Cerezo P, Viseras C, Caramella C, Applied Clay Science 2007, 36, 22.
- [164]. Jung H, Kim H-M, Choy YB, Hwang S-J, Choy J-H, Applied Clay Science 2008, 40, 99.
- [165]. Li K, Wang S, Wen S, Tang Y, Li J, Shi X, Zhao Q, ACS Appl Mater Interfaces 2014, 6, 12328. [PubMed: 25000274]
- [166]. Wang S, Wu Y, Guo R, Huang Y, Wen S, Shen M, Wang J, Shi X, Langmuir 2013, 29, 5030. [PubMed: 23419072]
- [167]. Gonçalves M, Figueira P, Maciel D, Rodrigues J, Qu X, Liu C, Tomás H, Li Y, Acta biomaterialia 2014, 10, 300. [PubMed: 24075886]
- [168]. Fraile JM, Garcia-Martin E, Gil C, Mayoral JA, Pablo LE, Polo V, Prieto E, Vispe E, Eur J Pharm Biopharm 2016, 108, 83. [PubMed: 27594212]
- [169]. Ghadiri M, Hau H, Chrzanowski W, Agus H, Rohanizadeh R, RSC Advances 2013, 3, 20193.

- [170]. Jung H, Kim H-M, Choy YB, Hwang S-J, Choy J-H, *Applied Clay Science* 2008, 40, 99.
- [171]. Ordikhani F, Dehghani M, Simchi A, *J Mater Sci Mater Med* 2015, 26, 269. [PubMed: 26507202]
- [172]. Dawson JI, Kanczler JM, Yang XB, Attard GS, Oreffo RO, *Adv Mater* 2011, 23, 3304; Gibbs DM, Black CR, Hulsart-Billstrom G, Shi P, Scarpa E, Oreffo RO, Dawson JI, *Biomaterials* 2016, 99, 16. [PubMed: 21661063]
- [173]. Carmeliet P, *Nat Med* 2000, 6, 1102; Nomi M, Miyake H, Sugita Y, Fujisawa M, Soker S, *Curr Stem Cell Res Ther* 2006, 1, 333; van Osch GJ, Mandl EW, Marijnissen WJ, van der Veen SW, Verwoerd-Verhoef HL, Verhaar JA, *Biorheology* 2002, 39, 215. [PubMed: 11017137]
- [174]. Dawson JI, Kanczler JM, Yang XB, Attard GS, Oreffo ROC, *Adv Mater* 2011, 23, 3304. [PubMed: 21661063]
- [175]. Gibbs DMR, Black CRM, Hulsart-Billstrom G, Shi P, Scarpa E, Oreffo ROC, Dawson JI, *Biomaterials* 2016, 99, 16. [PubMed: 27209259]
- [176]. Cross LM, Carrow JK, Ding X, Singh KA, Gaharwar AK, *Acs Appl Mater Inter* 2019.
- [177]. Howell DW, Peak CW, Bayless KJ, Gaharwar AK, *Advanced Biosystems* 2018, 1800092.
- [178]. Waters R, Alam P, Pacelli S, Chakravarti AR, Ahmed RPH, Paul A, *Acta Biomater* 2018, 69, 95; Waters R, Pacelli S, Maloney R, Medhi I, Ahmed RP, Paul A, *Nanoscale* 2016, 8, 7371. [PubMed: 29281806]
- [179]. Waters R, Alam P, Pacelli S, Chakravarti AR, Ahmed RPH, Paul A, *Acta Biomater* 2018, 69, 95. [PubMed: 29281806]
- [180]. Waters R, Pacelli S, Maloney R, Medhi I, Ahmed RP, Paul A, *Nanoscale* 2016, 8, 7371. [PubMed: 26876936]
- [181]. Chen W, Zuo H, Mahony TJ, Zhang B, Rolfe B, Xu ZP, *Sci Rep* 2017, 7, 13367; Chen W, Zhang B, Mahony T, Gu W, Rolfe B, Xu ZP, *Small* 2016, 12, 1627; Chen W, Zuo H, Rolfe B, Schembri MA, Cobbold RN, Zhang B, Mahony TJ, Xu ZP, *J Control Release* 2018, 292, 196. [PubMed: 29042573]
- [182]. Chen W, Zuo H, Rolfe B, Schembri MA, Cobbold RN, Zhang B, Mahony TJ, Xu ZP, *Journal of Controlled Release* 2018, 292, 196. [PubMed: 30414464]
- [183]. Chen W, Zuo H, Mahony TJ, Zhang B, Rolfe B, Xu ZP, *Scientific reports* 2017, 7, 13367. [PubMed: 29042573]
- [184]. Chen W, Zhang B, Mahony T, Gu W, Rolfe B, Xu ZP, *small* 2016, 12, 1627. [PubMed: 27000499]
- [185]. Schuldiner M, Yanuka O, Itskovitz-Eldor J, Melton DA, Benvenisty N, *Proc Natl Acad Sci U S A* 2000, 97, 11307; Wei TS, Ahn BY, Grotto J, Lewis JA, *Adv Mater* 2018, 30, e1703027. [PubMed: 11027332]
- [186]. Nagarajan N, Dupret-Bories A, Karabulut E, Zorlutuna P, Vrana NE, *Biotechnol Adv* 2018, 36, 521. [PubMed: 29428560]
- [187]. Chimene D, Lennox KK, Kaunas RR, Gaharwar AK, *Ann Biomed Eng* 2016, 44, 2090; Sears NA, Seshadri DR, Dhavalikar PS, Cosgriff-Hernandez E, *Tissue Eng Part B Rev* 2016, 22, 298. [PubMed: 27184494]
- [188]. Nagarajan N, Dupret-Bories A, Karabulut E, Zorlutuna P, Vrana NE, *Biotechnology Advances* 2018, 36, 521; Wang MO, Vorwald CE, Dreher ML, Mott EJ, Cheng MH, Cinar A, Mehdizadeh H, Somo S, Dean D, Brey EM, Fisher JP, *Adv Mater* 2015, 27, 138. [PubMed: 29428560]
- [189]. Truby RL, Lewis JA, *Nature* 2016, 540, 371; Ober TJ, Foresti D, Lewis JA, *Proc Natl Acad Sci U S A* 2015, 112, 12293; Liu X, Yuk H, Lin S, Parada GA, Tang TC, Tham E, de la Fuente-Nunez C, Lu TK, Zhao X, *Adv Mater* 2018, 30, 1704821. [PubMed: 27974748]
- [190]. Hong S, Sycks D, Chan HF, Lin S, Lopez GP, Guilak F, Leong KW, Zhao X, *Adv Mater* 2015, 27, 4035. [PubMed: 26033288]
- [191]. Okamoto M, Nam PH, Maiti P, Kotaka T, Hasegawa N, Usuki A, *Nano Letters* 2001, 1, 295; Rodriguez MJ, Dixon TA, Cohen E, Huang W, Omenetto FG, Kaplan DL, *Acta Biomater* 2018, 71, 379.
- [192]. Wilson SA, Cross LM, Peak CW, Gaharwar AK, *Acs Appl Mater Inter* 2017, 9, 43449.

- [193]. Zhai X, Ruan C, Ma Y, Cheng D, Wu M, Liu W, Zhao X, Pan H, Lu WW, *Advanced Science* 2017.
- [194]. Zhai X, Ma Y, Hou C, Gao F, Zhang Y, Ruan C, Pan H, Lu WW, Liu W, *ACS Biomaterials Science & Engineering* 2017, 3, 1109.
- [195]. Chimene D, Peak CW, Gentry JL, Carrow JK, Cross LM, Mondragon E, Cardoso GB, Kaunas R, Gaharwar AK, *ACS Appl Mater Interfaces* 2018, 10, 9957. [PubMed: 29461795]
- [196]. Chimene D, Peak CW, Gentry JL, Carrow JK, Cross LM, Mondragon E, Cardoso GB, Kaunas R, Gaharwar AK, *Acs Appl Mater Inter* 2018, 10, 9957.
- [197]. Jin Y, Compaan A, Chai W, Huang Y, *ACS Appl Mater Interfaces* 2017, 9, 20057. [PubMed: 28534614]
- [198]. Ding H, Chang R, *Applied Sciences* 2018, 8, 403.
- [199]. Jin Y, Compaan A, Chai W, Huang Y, *Acs Appl Mater Inter* 2017, 9, 20057.
- [200]. Jin Y, Chai W, Huang Y, *Mater Sci Eng C Mater Biol Appl* 2017, 80, 313. [PubMed: 28866170]
- [201]. Rodriguez MJ, Dixon TA, Cohen E, Huang W, Omenetto FG, Kaplan DL, *Acta Biomater* 2018, 71, 379. [PubMed: 29550442]
- [202]. Jin Y, Chai W, Huang Y, *Materials Science and Engineering: C* 2017, 80, 313. [PubMed: 28866170]
- [203]. Jin Y, Shen Y, Yin J, Qian J, Huang Y, *ACS Appl Mater Interfaces* 2018, 10, 10461. [PubMed: 29493213]
- [204]. Sydney Gladman A, Matsumoto EA, Nuzzo RG, Mahadevan L, Lewis JA, *Nature Materials* 2016, 15, 413. [PubMed: 26808461]
- [205]. Guo J, Zhang R, Zhang L, Cao X, *ACS Macro Letters* 2018, 7, 442.
- [206]. Jin Y, Shen Y, Yin J, Qian J, Huang Y, *Acs Appl Mater Inter* 2018, 10, 10461.
- [207]. Wang Y, Cui W, Chou J, Wen S, Sun Y, Zhang H, *Colloids and Surfaces B: Biointerfaces* 2018, 172, 90. [PubMed: 30142529]
- [208]. Carrow JK, Di Luca A, Dolatshahi-Pirouz A, Moroni L, Gaharwar AK, *Regenerative Biomaterials* 2018, 6, 29. [PubMed: 30740240]



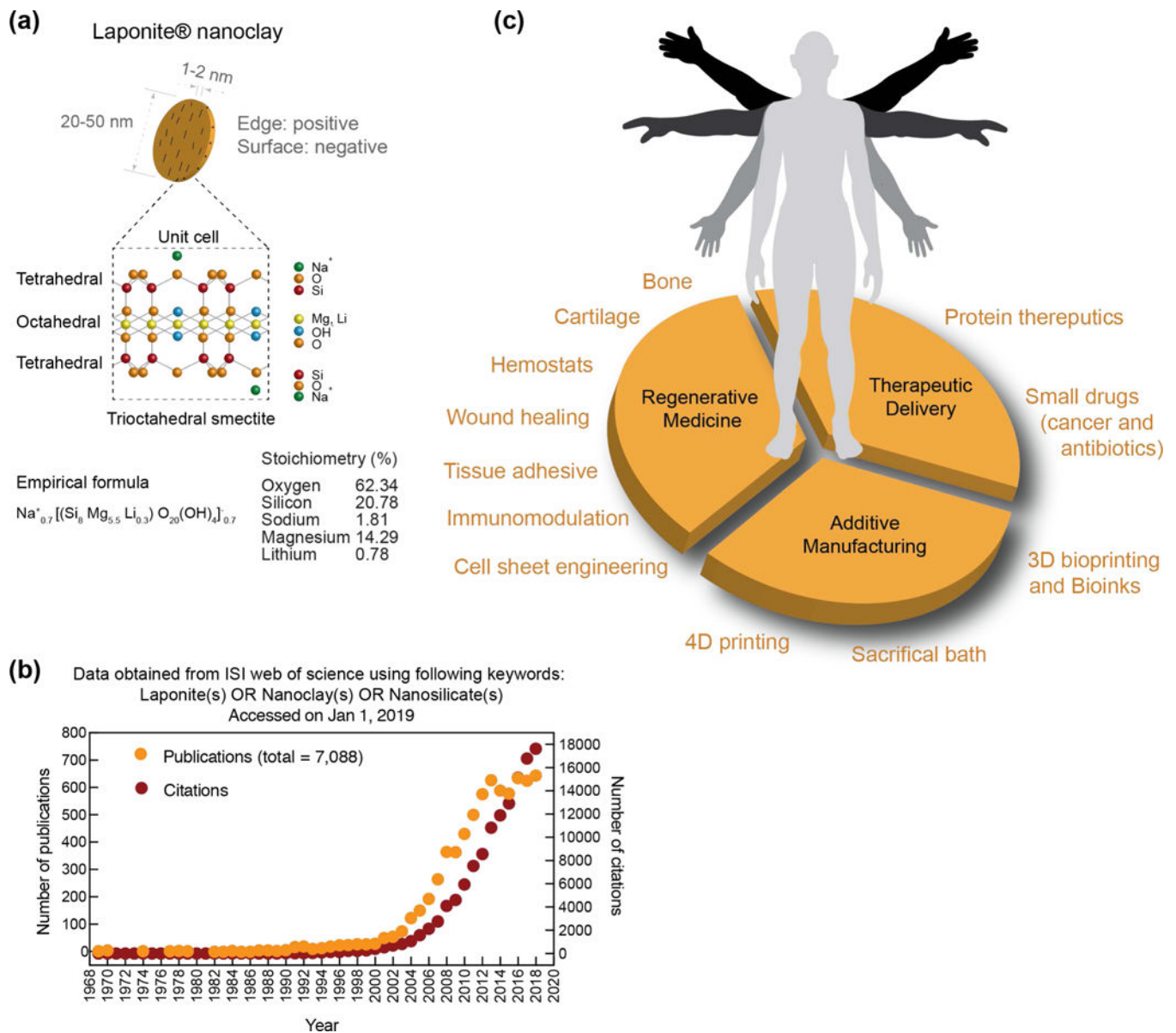


**Figure 1. Nanoclay in biomedical engineering.**

(a) Size, shape and chemical composition of individual nanoclay. (b) Exponential increase in investigating nanoclay for various applications. Data obtained from ISI web of science using Laponite(s)/nanoclay(s)/nanosilicates(s) (01 Jan 2019). (c) Biomedical applications of nanoclay are investigated in regenerative medicine, therapeutic delivery and additive manufacturing.

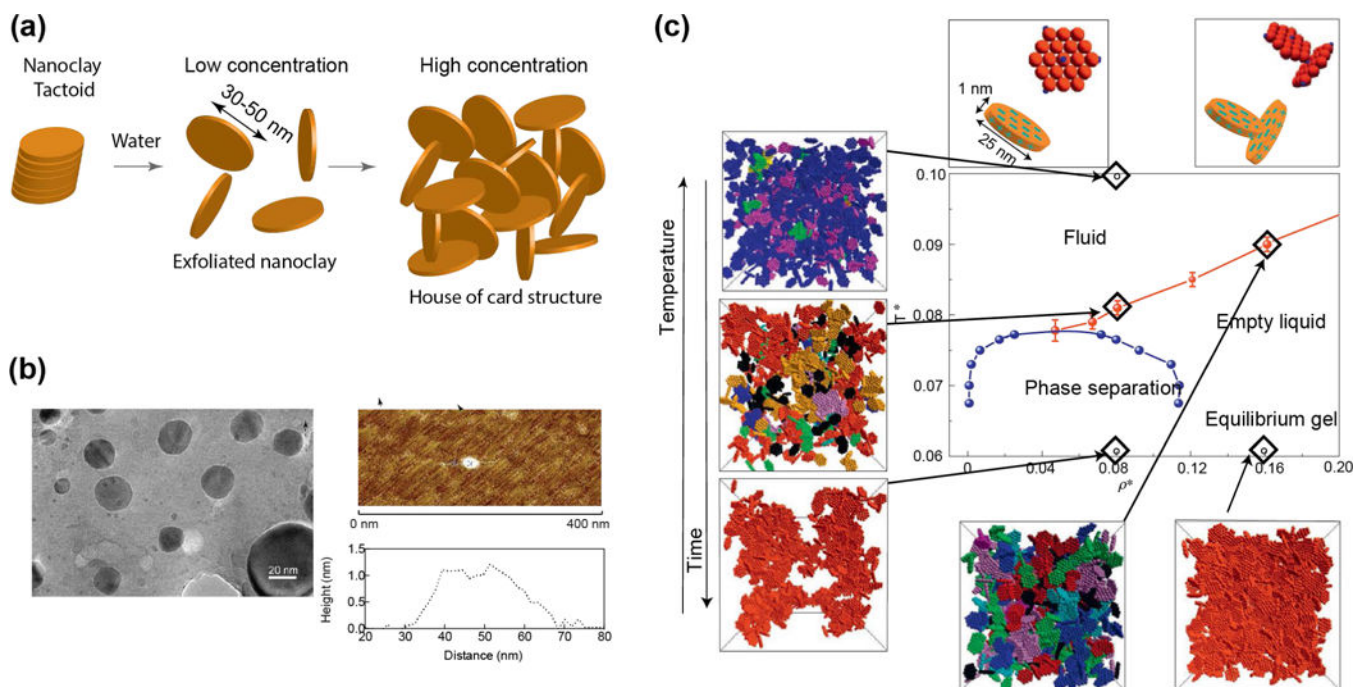


**Figure 2. Physicochemical characteristics of nanoclay.**

(a) Schematic showing exfoliation of nanoclay. At high concentration of nanoclay >3wt%, house-of-card structure is formed that results in formation of gel. (b) Size and shape of individual nanoclay. TEM show circular morphology of individual nanoclay with diameter ~30–50nm, while AFM show thickness of individual nanoclay ~1–2nm. Adapted with permission<sup>[13]</sup> Copyright © National Academy of Sciences. (c) Phase diagram of nanoclay demonstrate formation of sol-gel transition with respect to concentration, temperature, and time. Adapted with permission<sup>[26]</sup> Copyright © Springer Nature Publishing AG.

## Stability of nanoclay in physicochemical conditions

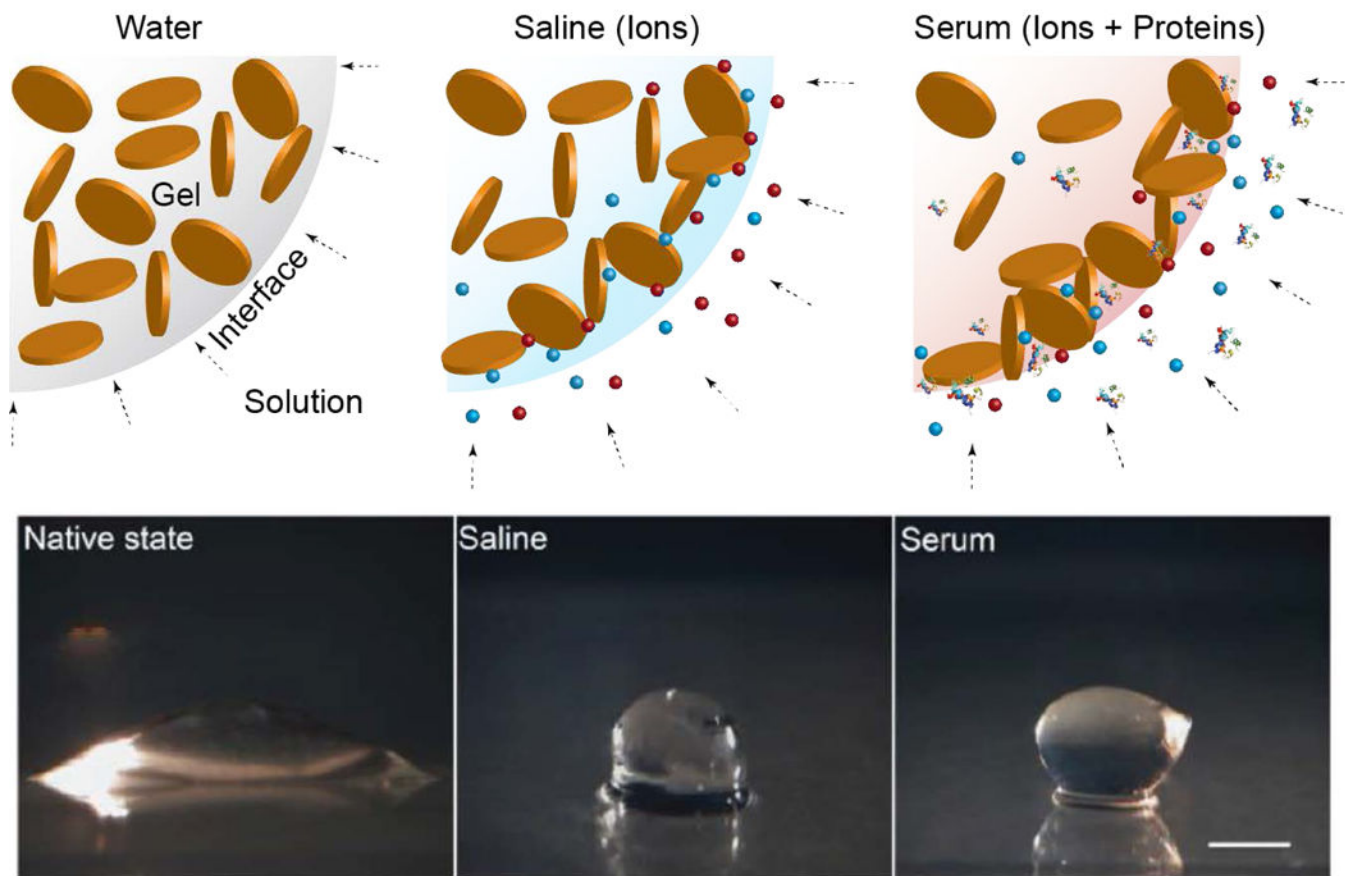


**Figure 3. Interaction of exfoliated nanoclay with water, saline and serum.**

Stability of nanoclay gel in physiological conditions such as water, saline and serum.

Adapted and redrawn with permission<sup>[95]</sup> Copyright © John Wiley & Sons, Inc.

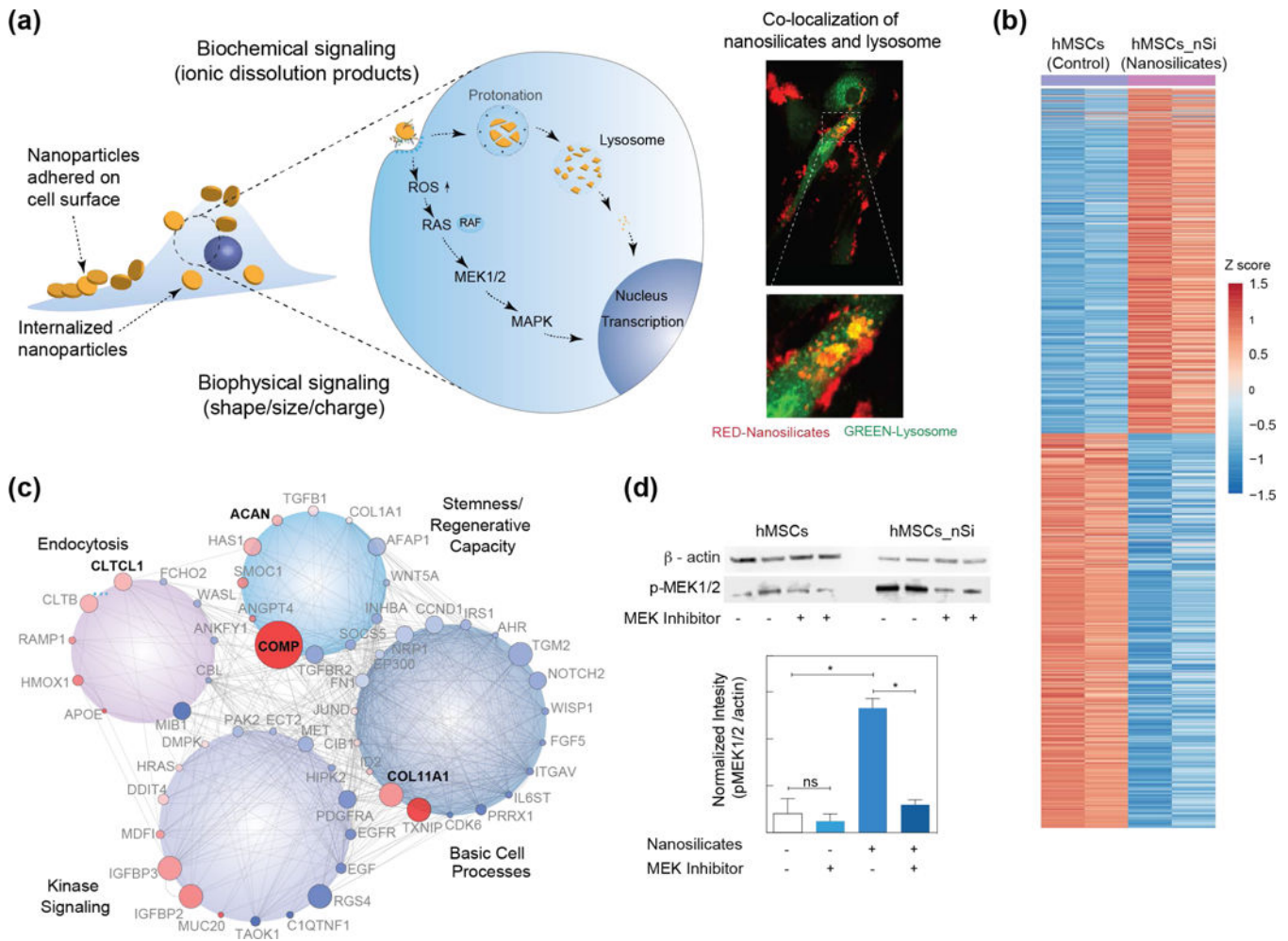


**Figure 4. Interactions of nanoclay with cells.**

(a) Schematic showing interaction of nanoclay with cells. Nanoclay induces both biophysical and biochemical signaling on cells. Co-localization of nanoclay and lysosome within hMSCs (Red – nanoclay; Green – lysosome) determine using microscopy. (b) Normalized gene expression of >4,000 genes following treatment with nanoclay ( $p_{\text{adjust}} < 0.05$ , red (up-regulated): 1,897 genes; blue (down-regulated): 2,171 genes). (c) Gene network of differentially regulated genes after nanoclay treatment. (d) Western blot analysis established role of MAPK/ERK signaling after treatment with nanoclay and MEK inhibitor. Adapted and modified with permission<sup>[13]</sup> Copyright © National Academy of Sciences.

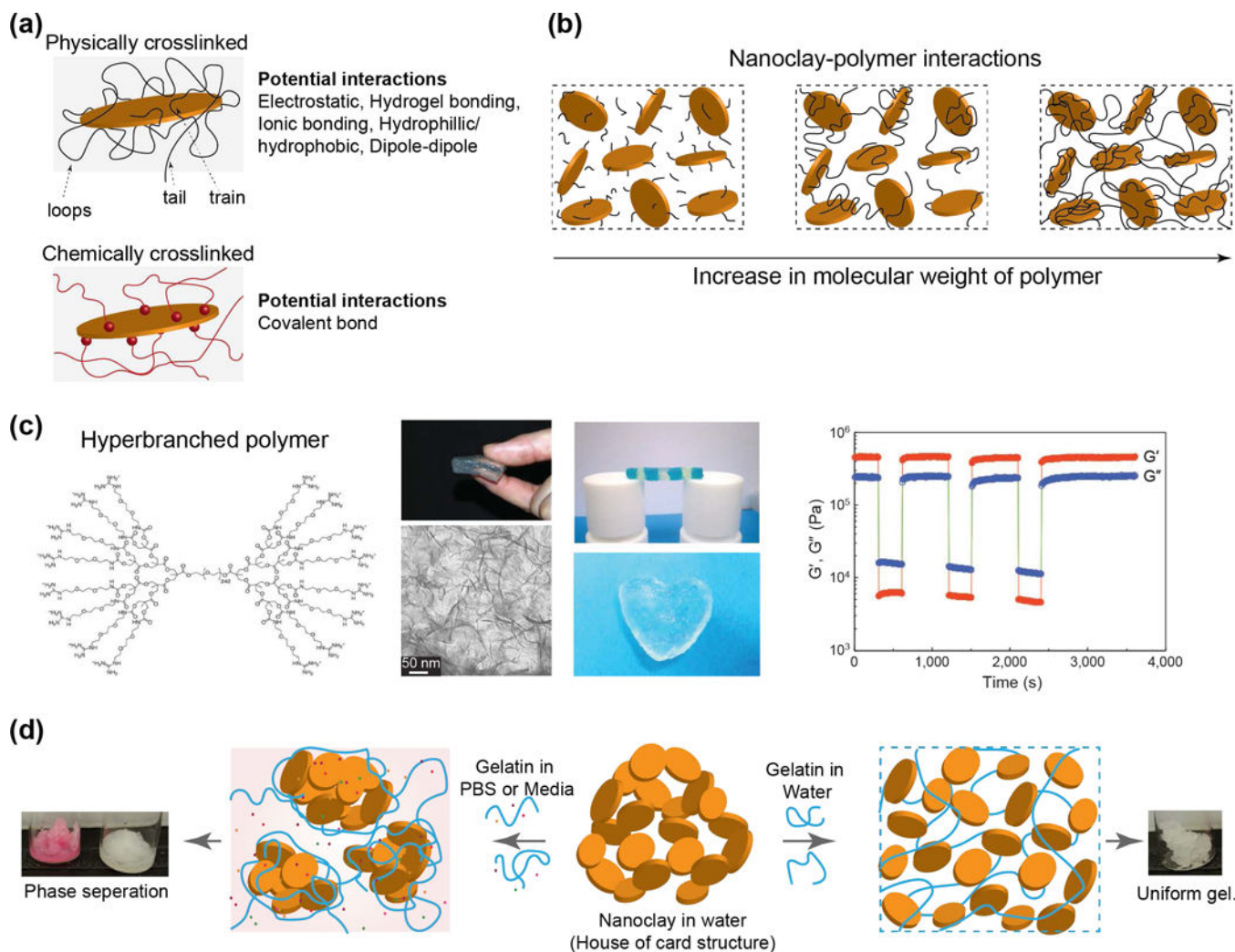


**Figure 5. Interactions of nanoclay with polymers.**

(a) Nanoclay can form both physical and chemical bonds with polymer chains via multiple mechanisms. (b) Nanoclay interactions with polymer with different molecular weight. Critical size of polymer chain result in formation of physically crosslinked network. (c) Formation of self-assembled gel when nanoclay is mixed with polymeric binder (hyperbranched polymer). Polymer end group interact with nanoclay and result in formation of mechanically stable hydrogels. Adapted with permission<sup>[71]</sup> Copyright © Springer Nature Publishing AG. (d) Effect of ions on the stability of hydrogels. Adapted and modified with permission<sup>[92]</sup> Copyright © Royal Society of Chemistry.

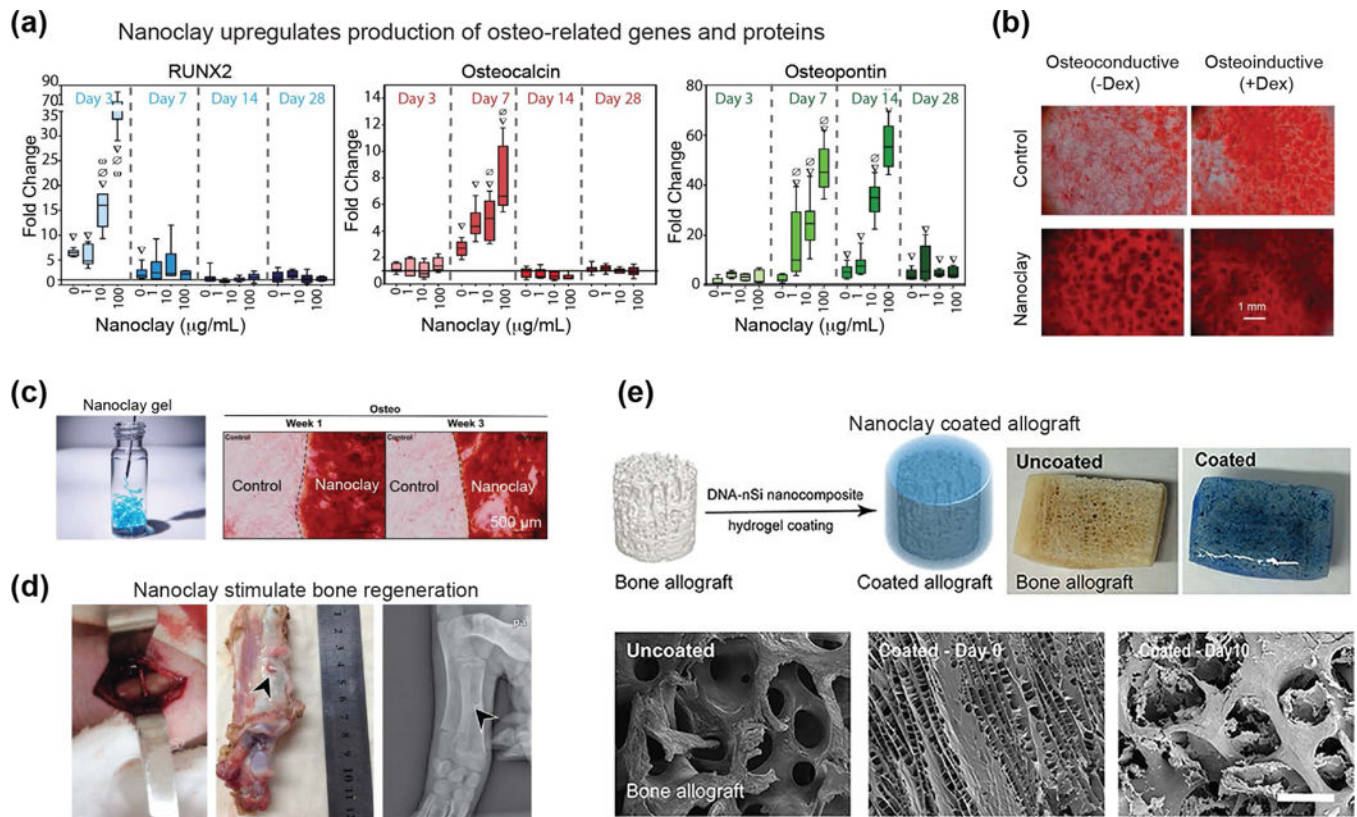


**Figure 6. Osteoinductive characteristics of nanoclay.**

(a) Nanoclay treatment in human adipose derived stem cells (hASCs) results in dose-dependent increase in osteo-related gene expression (RUNX2, osteocalcin, and osteopontin). Adapted with permission<sup>[55]</sup> Copyright © Elsevier. (b) Human mesenchymal stem cells (hMSCs) treated with increasing concentrations of nanoclay produced mineralized matrix in osteoconductive and osteoinductive media. Adapted with permission<sup>[54]</sup> Copyright © John Wiley & Sons, Inc. (c) Nanoclay gel support adhesion of stem cells and induce osteogenic differentiation as determined by alizarin red staining. Adapted with permission<sup>[95]</sup> Copyright © John Wiley & Sons, Inc. (d) In vivo bone regeneration is demonstrated by using nanoclay scaffolds. Adapted with permission<sup>[96]</sup> PLOS ONE. (e) Allograft can be coated with nanoclay-based gels to promote bone formation. Adapted with permission<sup>[106]</sup> Copyright © American Chemical Society.

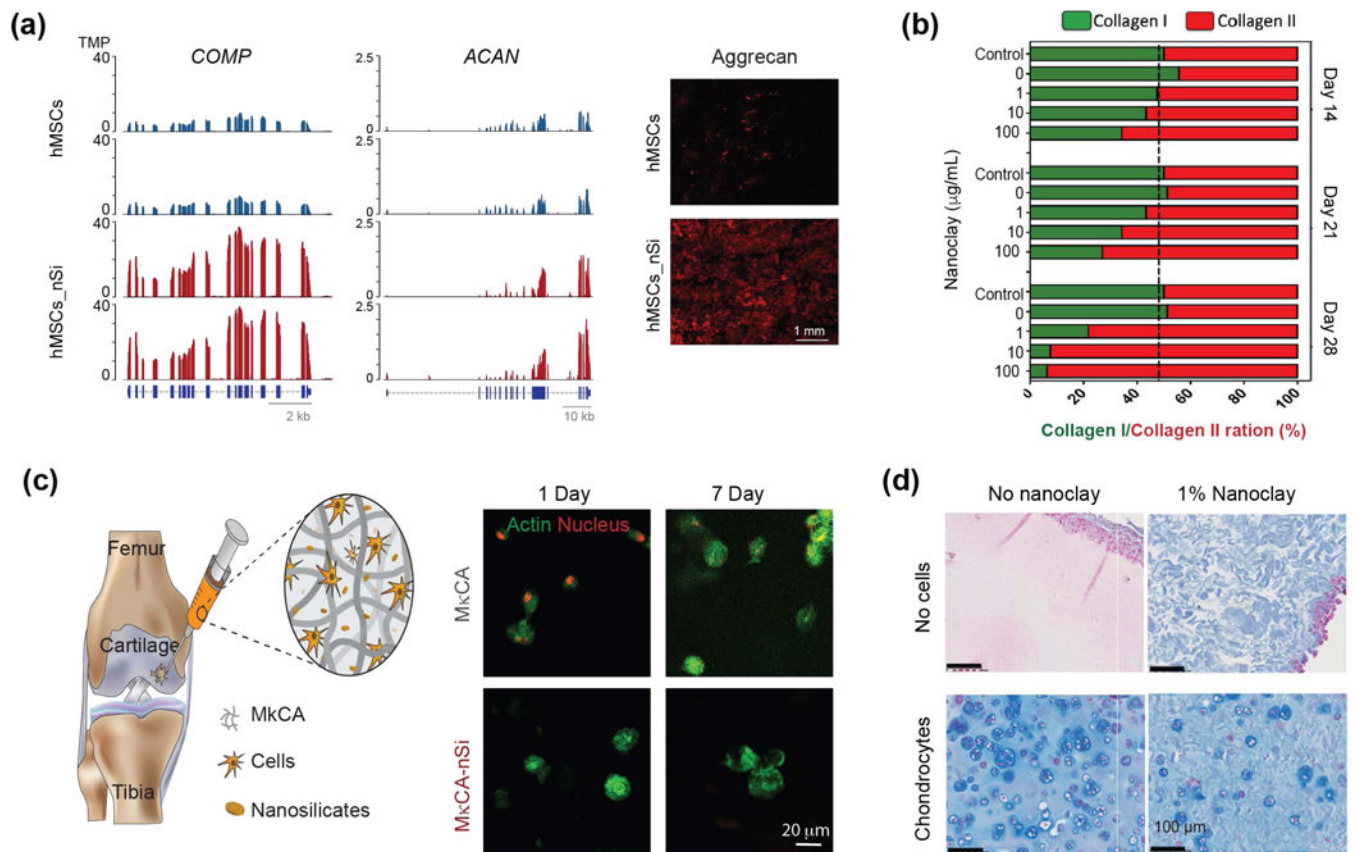


**Figure 7. Nanoclay promote formation of cartilage-related proteins.**

(a) Significant upregulation of cartilage related genes such as COMP and ACAN are observed after nanoclay treatment of hMSCs. After 21 days, significant production of ACAN and GAGs are observed from western blot. Adapted with permission<sup>[13]</sup> Copyright © National Academy of Sciences. (b) Stem cells treated with nanoclay results in enhanced production of collagen II, which is important component of cartilaginous ECM. Adapted with permission<sup>[55]</sup> Copyright © Elsevier. (c) Nanoclay loaded hydrogels are used for delivery of stem cells for cartilage regeneration. Encapsulated cells show high viability and assume round shape morphology after 7 days indicating potential application in cartilage regeneration. Adapted and modified with permission<sup>[114]</sup> Copyright © Royal Society of Chemistry. (d) Nanoclay loaded in silated hydroxypropylmethyl cellulose showed enhanced production of cartilaginous ECM as demonstrated by Alcian blue staining by encapsulated chondrocytes. Adapted with permission<sup>[117]</sup> Copyright © Elsevier.

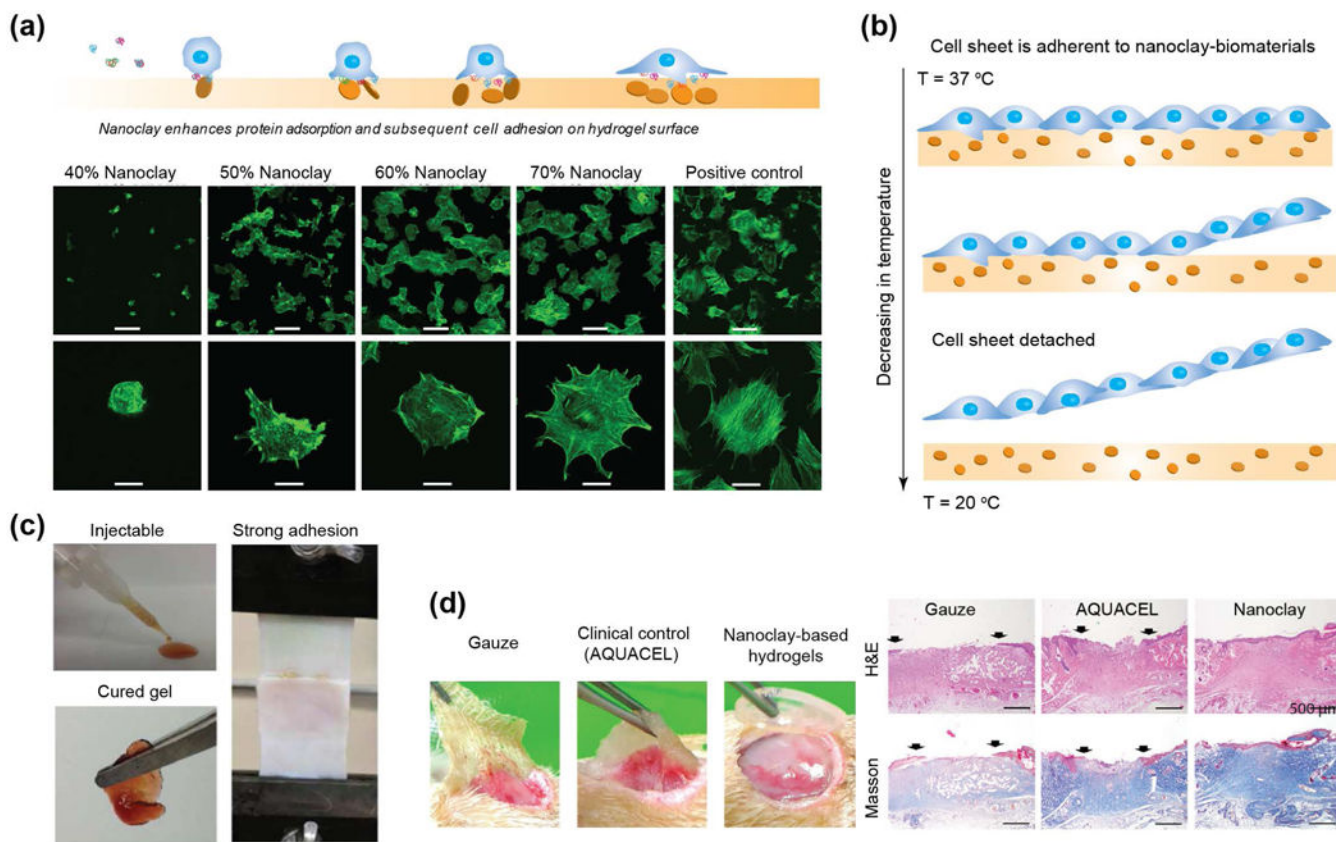


**Figure 8. Nanoclay support cell and tissue adhesion.**

(a) The addition of nanoclay to a non-fouling polymer (PEO) results in enhanced cell adhesion and spreading. Adapted and modified with permission<sup>[98]</sup> Copyright © Elsevier.

(b) Concept of cell sheet engineering using nanoclay and thermoresponsive polymer.

(c) Dopamine-modified multi-armed PEG (PEG-D) mixed with nanoclay was developed as tissue adhesive. Injectability combined with wet tissue adhesion allow this fit-to-shape sealant to be used as an injectable bandage. Adapted with permission<sup>[134]</sup> Copyright © American Chemical Society.

(d) nanoclay-based hydrogels facilitate complete closure in normal and diabetic wounds. Re-epithelialization and formation of new connective tissues was observed when nanoclay-based hydrogel are used as wound healing patch. Adapted with permission<sup>[145]</sup> Copyright © Royal Society of Chemistry.



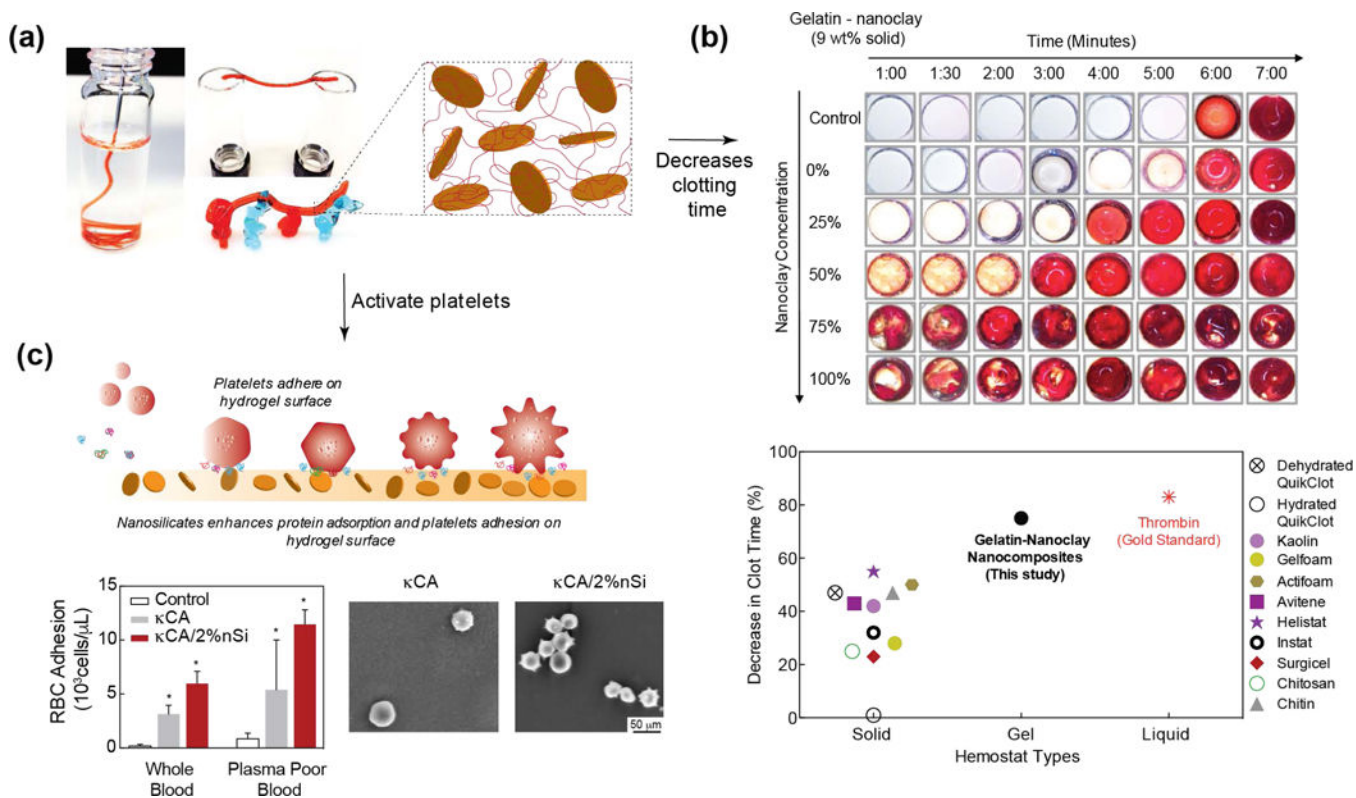


**Figure 9. Hemostatic ability of nanoclay-based biomaterials.**

(a) The addition of nanoclay to gelatin results in shear-thinning hydrogels. The force required to shear-thinning (yield stress) can be modulated by changing gelatin to nanoclay concentration and ratio. Addition of nanoclay results in shear-recovery of hydrogel network. (b) In vitro studies show that that addition of nanoclay reduces the clotting time by ~70%, which is similar to thrombin. Adapted and modified with permission<sup>[147]</sup> Copyright © American Chemical Society. (c) Nanoclay enhance protein and cell adhesion that also result in activation of platelets and induces rapid clotting. Adapted and modified with permission<sup>[150]</sup> Copyright © Elsevier.

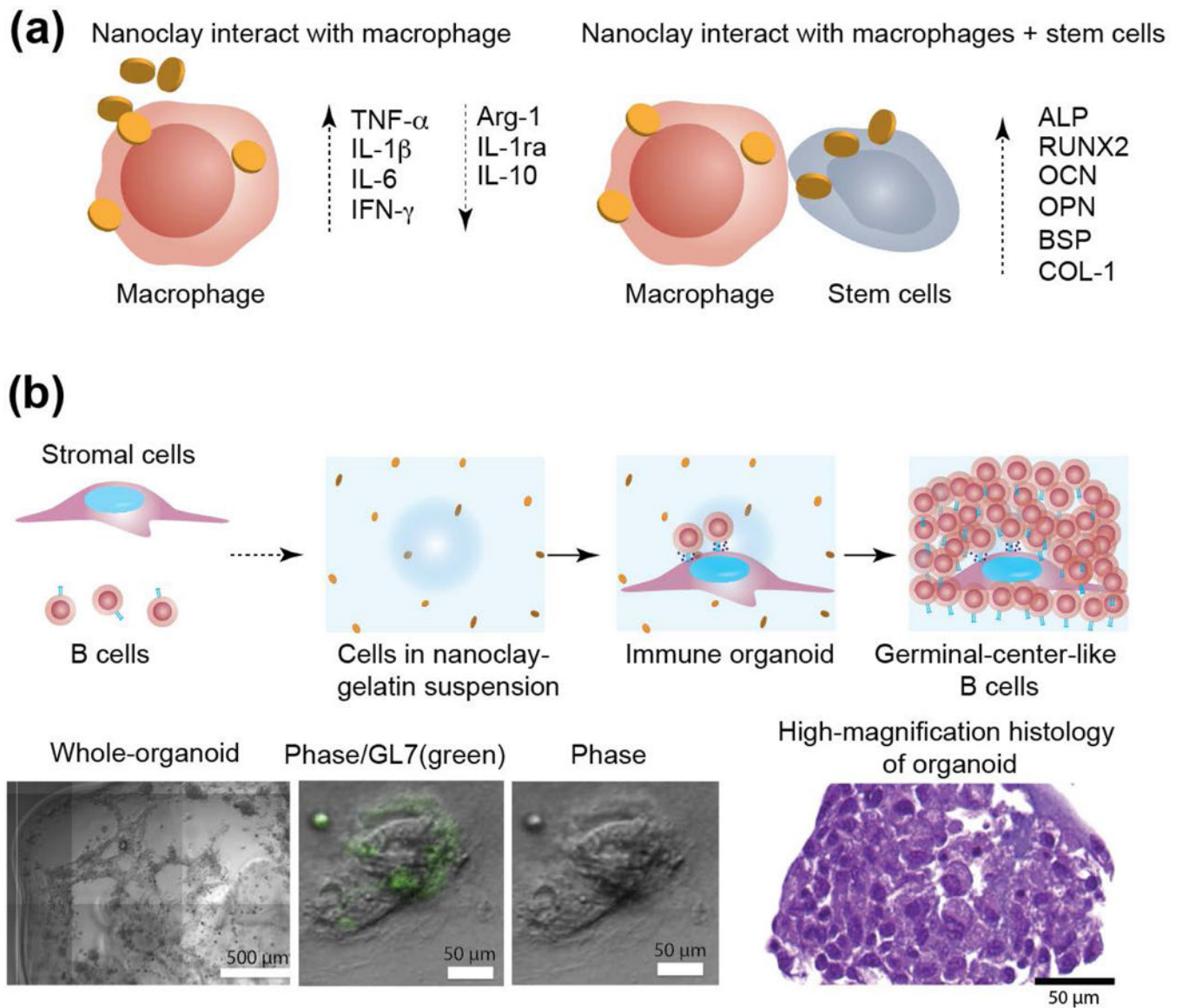


**Figure 10. Immunomodulation characteristics of nanoclay.**

(a) Nanoclay induce a phenotypic switch in macrophages in presence of stem cells. The addition of nanoclay to macrophages results in a decrease in anti-inflammatory factors (IL-1ra, IL-10, and Arg-1) and an increase in pro-inflammatory factors (TNF- $\alpha$ , IL-1 $\beta$ , IL-6, and IFN- $\gamma$ ). Nanoclay cultured with macrophages and rBMSCs result in significant upregulation of osteo-related gene (ALP, RUNX2, OCN, OPN, BSP and COL-1). (b) Nanoclay-based hydrogels are used to obtain immune organoids. Image show 3D immune organoids containing naive B cells and BALB/c 3T3 fibroblasts transduced with CD40L. Close-up image show organoid staining of GL7 antibody. H&E-stained sections of B cells in immune organoids. Adapted and modified with permission<sup>[158]</sup> Copyright © Elsevier.

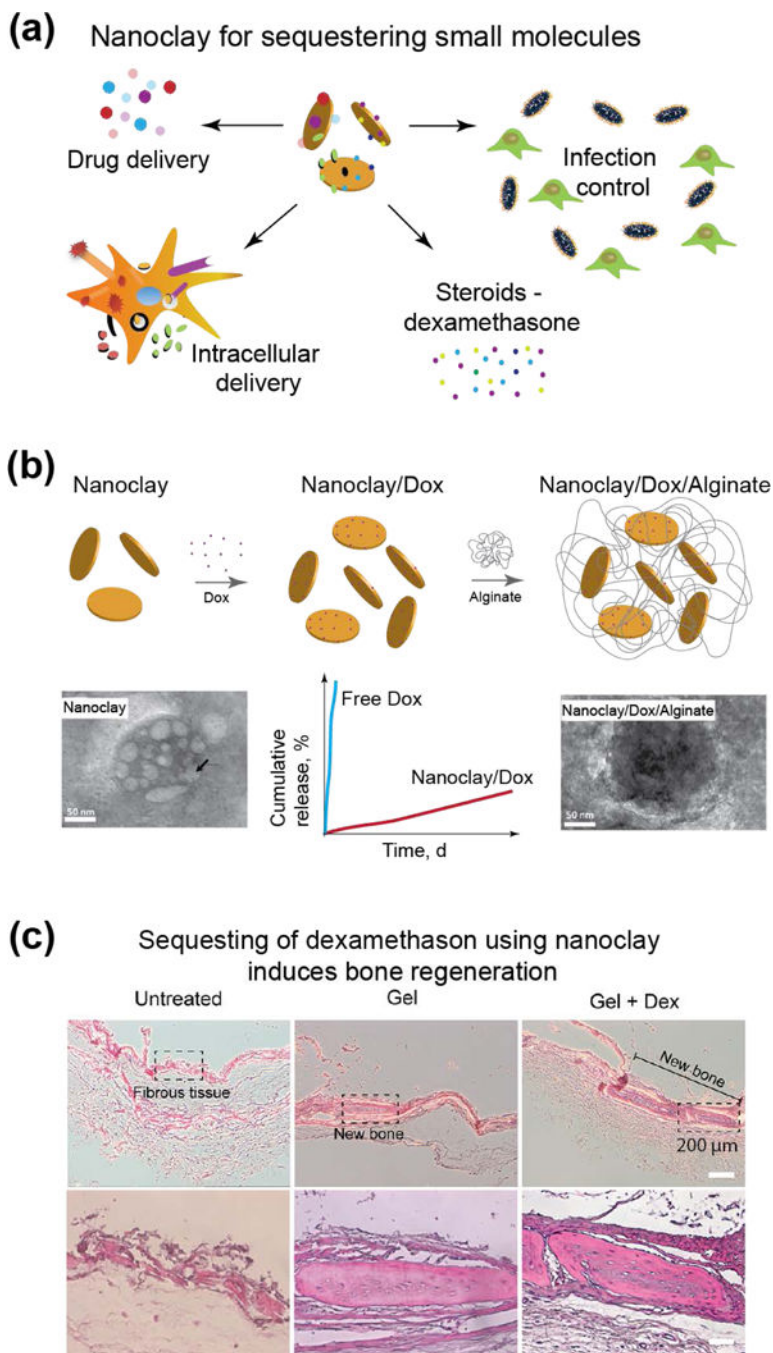


**Figure 11. Nanoclay for sustained delivery of small molecules.**

(a) Small molecules sequestered and delivered using nanoclay. (b) Nanoclay/doxorubicin complexes coated with alginate to enhance cellular uptake. Addition of nanoclay result in sustained release over 21 days. Adapted with permission<sup>[167]</sup> Copyright © Elsevier. (c) Nanoclay-based hydrogels loaded with dexamethasone showed enhanced bone formation. Adapted with permission<sup>[106]</sup> Copyright © American Chemical Society.

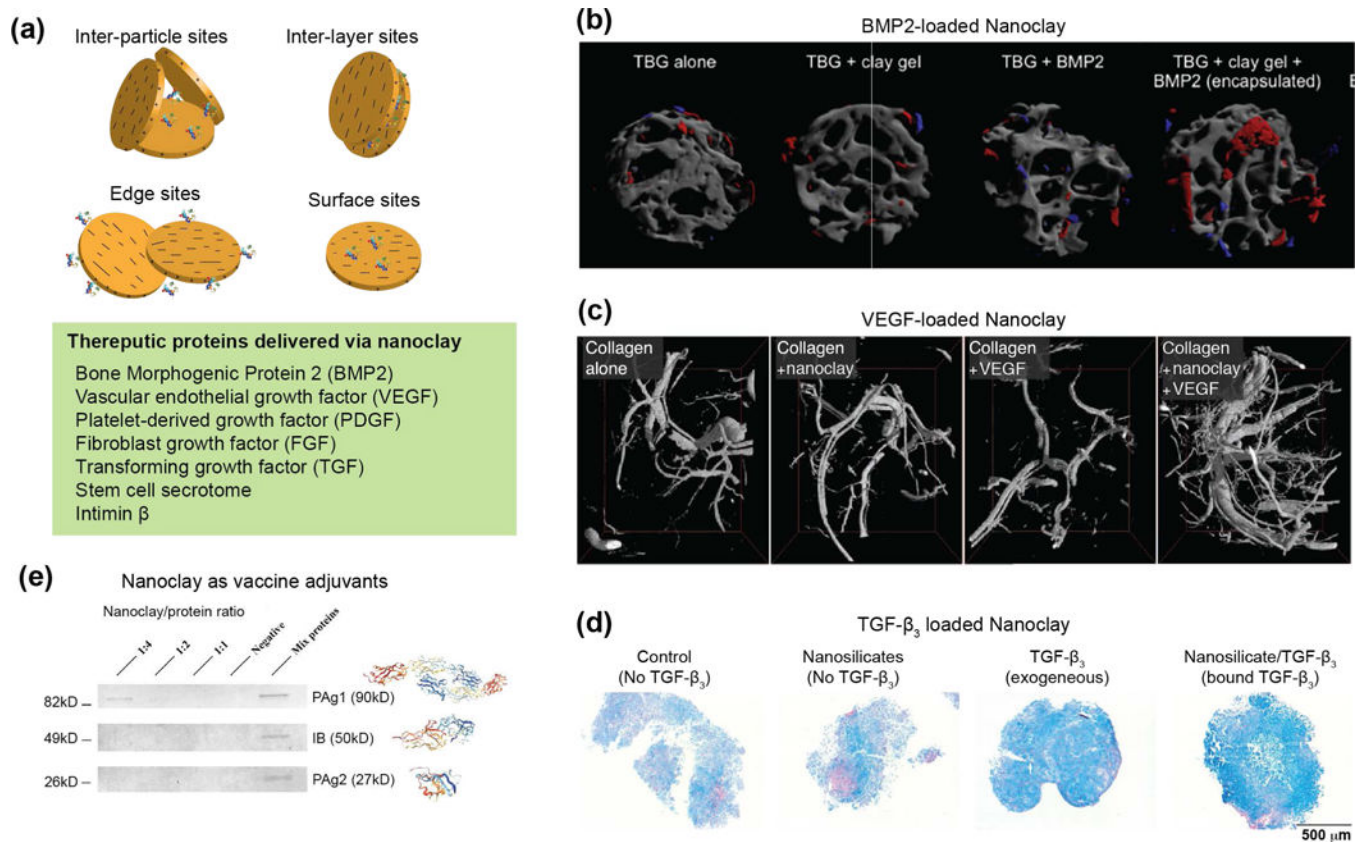


**Figure 12. Nanoclay for delivery of protein therapeutics.**

(a) Interaction of nanoclay with protein therapeutics. The charged characteristics of nanoclay results sequestering proteins in at different sites. (b) Trabecular bone graft (TBG) loaded with nanoclay gel and BMP2 induced robust bone formation. Red area shows formation of new bone. Sustained and prolong delivery of BMP2 using nanoclay can reduce effective concentration of BMP2 by 10–100 folds compared to other studies. Adapted with permission<sup>[175]</sup> Copyright © Elsevier. (c) Collagen gel loaded with nanoclay and VEGF induces formation of new blood vessels. An increase in vessel number and volume are increased due to delivery of nanoclay/VEGF. Adapted with permission<sup>[174]</sup> Copyright © John Wiley & Sons, Inc. (d) Delivery of TGF-beta sequester on nanoclay induces chondrogenic differentiation of bone marrow stem cells. Adapted with permission<sup>[176]</sup> Copyright © American Chemical Society. (e) Nanoclay sequester multiple vaccine adjuvants to induce robust immune response. Adapted with permission<sup>[182]</sup> Copyright © Elsevier.

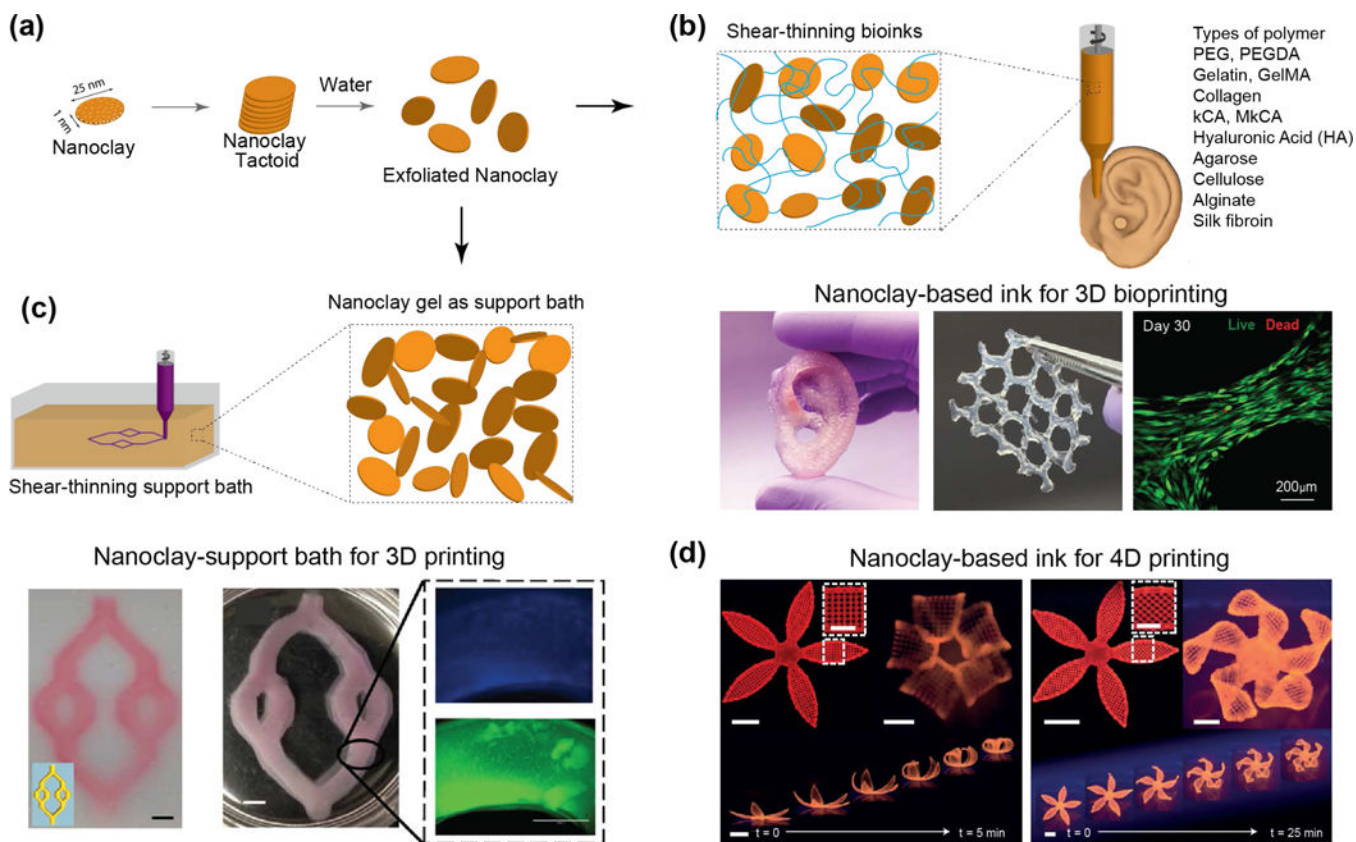


**Figure 13. Nanoclay in additive manufacturing.**

(a) The addition of exfoliated nanoclay to various polymers at low concentrations enables for shear-thinning bioinks. (b) Nanoclay-based ink for 3D bioprinting. The addition of nanoclay to GelMA-kCA bioink improved the mechanical properties *via* ionic-covalent entanglements. Such reinforcements demonstrated improved extrusion of complex scaffolds while supporting high cell viability in bioprinted structures (> 90%). Adapted with permission<sup>[196]</sup> Copyright © American Chemical Society. (c) Nanoclay-support bath for 3D printing. The rapid recoverability and transparent properties enables nanoclay-based gels for precise construction of printed geometries and solidification of geometries upon the application of a suitable crosslinking mechanism. Adapted with permission<sup>[199]</sup> Copyright © American Chemical Society. (d) Nanoclay-based ink for 4D printing. The addition of nanoclay consents for precise deposition with shear-induced anisotropic orientations allowing for a programmed response to an external stimulus to mimic the functional folding of a flower architecture. Adapted with permission<sup>[204]</sup> Copyright © Springer Nature Publishing AG.